PHILOSOPHICAL TRANSACTIONS OF THE ROYAL SOCIETY B BIOLOGICAL SCIENCES

Structure and function of the Nautilus statocyst

H. Neumeister and B. U. Budelmann

Phil. Trans. R. Soc. Lond. B 1997 **352**, 1565-1588
doi: 10.1098/rstb.1997.0142

Structure and function of the *Nautilus* statocyst

H. NEUMEISTER[1*]† AND B. U. BUDELMANN[1,2]

[1]*Marine Biomedical Institute,* [2]*Department of Otolaryngology, University of Texas Medical Branch, Galveston, TX 77555-1163, USA*

This paper is dedicated to Professor John Z. Young, FRS, FBA, on the occasion of his 90th birthday

CONTENTS

		PAGE
1.	Introduction	1565
2.	Materials and methods	1566
3.	Results	1569
4.	Discussion	1581
	References	1586

SUMMARY

The two equilibrium receptor organs (statocysts) of *Nautilus* are ovoid sacks, half-filled with numerous small, free-moving statoconia and half with endolymph. The inner surface of each statocyst is lined with 130 000–150 000 primary sensory hair cells. The hair cells are of two morphological types. Type *A* hair cells carry 10–15 kinocilia arranged in a single ciliary row; they are present in the ventral half of the statocyst. Type *B* hair cells carry 8–10 irregularly arranged kinocilia; they are present in the dorsal half of the statocyst. Both type of hair cells are morphologically polarized. To test whether these features allow the *Nautilus* statocyst to sense angular accelerations, behavioural experiments were performed to measure statocyst-dependent funnel movements during sinusoidal oscillations of restrained *Nautilus* around a vertical body axis. Such dynamic rotatory stimulation caused horizontal phase-locked movements of the funnel. The funnel movements were either in the same direction (compensatory funnel response), or in the opposite direction (funnel follow response) to that of the applied rotation. Compensatory funnel movements were also seen during optokinetic stimulation (with a black and white stripe pattern) and during stimulations in which optokinetic and statocyst stimulations were combined.

These morphological and behavioural findings show that the statocysts of *Nautilus*, in addition to their function as gravity receptor organs, are able to detect rotatory movements (angular accelerations) without the specialized receptor systems (crista/cupula systems) that are found in the statocysts of coleoid cephalopods. The findings further indicate that both statocyst and visual inputs control compensatory funnel movements.

1. INTRODUCTION

Equilibrium receptor organs provide information about body position and movement in the three dimensions of space and are involved in the control of static and dynamic compensatory reflexes. Depending upon life styles and habitats, different animals have different requirements for equilibrium receptor organs. In general, fast moving species orient themselves with respect to the direction of gravity (and other linear accelerations), as well as respond to rotatory body movements (angular accelerations). Consequently, their equilibrium receptor organs include two morphologically and physiologically different receptor systems: a gravity receptor system for the detection of position relative to the direction of gravity, and an angular acceleration receptor system for the detection of rotatory movements.

In invertebrates, the ability to distinguish between linear and angular accelerations is known in arthropods (decapod crustaceans and some insects) as well as in higher cephalopod molluscs (Markl 1974; Budelmann 1976, 1988; Sandeman 1976, 1983). In fast moving coleoid cephalopods, such as octopuses, cuttlefish and squids, orientation with respect to gravity and angular accelerations is well known and their equilibrium receptor organs (statocysts) include receptor systems for the detection of gravity and angular accelerations (Young 1960; Budelmann *et al.* 1987*a*; Budelmann 1990). As in vertebrates, information from these two systems is centrally integrated with visual and proprioceptive informations to optimize equilibrium control, such as during compensatory eye movements (including postrotatory nys-

* Author for correspondence.
† Present address: Hopkins Marine Station, Stanford University, Pacific Grove, CA 93950-3094, USA (heike@leland.stanford.edu).

tagmus) and compensatory head and body movements (Budelmann 1970, 1990; Collewijn 1970; Messenger 1970; Budelmann & Young 1984; Preuss & Budelmann 1995*a*).

In contrast to coleoid cephalopods, very little is known about equilibrium orientation and the statocysts of *Nautilus*. Early light microscopical studies showed that their structure is not as complex as that of coleoid cephalopods (MacDonald 1855, 1857; Griffin 1897; Young 1965) but rather similar to that of gastropods and bivalves (Budelmann 1975, 1988). The *Nautilus* statocyst does not show the coleoid differentiation into gravity and angular acceleration receptor systems (Young 1965), i.e. confined sensory epithelia (maculae with statolith/statoconia and cristae with cupulae) are missing. Consequently, the *Nautilus* statocyst was considered to be a gravity receptor organ only (Budelmann 1975). Young (1965) mentioned the possibility of angular acceleration reception for the *Nautilus* statocyst but did not provide morphological or physiological evidences for his idea.

Nautilus locomotes by jet propulsion but, compared to coleoid cephalopods, is rather slow moving (Wells 1990). Due to the arrangement of the gas-filled chambers of the shell, the animal's centre of buoyancy lies above the centre of gravity and, consequently, *Nautilus* is stabilized in pitch and roll. During locomotion, jet propulsion causes pendulum-like pitch movements; these include changes of position of the animal with respect to gravity and are described as 'rocking' (Hartline *et al.* 1979; Chamberlain 1987). The compensatory eye movements that occur during rocking are known to depend on the animal's position relative to gravity and thus are statocyst controlled (Hartline *et al.* 1979). In addition, during passive rotations around roll and pitch axes compensatory funnel movements were seen to occur in a direction opposite to the direction of the passive movement (Packard *et al.* 1980). This is an indication that *Nautilus* might be sensitive to rotatory movements (angular accelerations).

The aims of this study are to describe the structure of the *Nautilus* statocyst at light and electron microscopical levels and to use behavioural experiments (measurements of funnel movements during sinusoidal oscillations) to investigate a possible sensitivity of *Nautilus* to horizontal rotatory movements (horizontal angular accelerations).

2. MATERIALS AND METHODS

(*a*) *Experimental animals*

Nine *Nautilus pompilius* L. (females and males), imported from the Philippines via a commercial dealer, were used in this study (maximum shell diameter 90–140 mm; weight 330–495 g). The animals were maintained in two circular tanks (1 m diameter, 40 cm high; water volume 350 l; for further details, see Yang *et al.* (1989)) in a closed system of recirculating artificial seawater (salinity 35–36‰; pH 8.0–8.4; ammonia nitrogen max. 0.05‰; nitrite nitrogen max. 0.2‰; nitrate nitrogen max. 20‰; trace elements added) at a temperature of 15–18 °C. Illumination was kept at 0.35 lux (red light) or 0.17 lux (no room light). Occasionally white light (22 lux) was used. The animals were fed dead fish or shrimp three times per week.

(*b*) *Anatomical analysis of the statocysts*

Three animals were used for the structural analysis of the statocysts. In addition, four statocysts were available from animals sacrificed and fixed in this laboratory already in 1988. The structure was analysed by light (LM), scanning (SEM), and transmission electron microscopy (TEM). For dissection of the statocysts, animals were anaesthetized by cooling to 5 °C in a magnesium chloride solution (7.5% magnesium chloride [$MgCl_2 \times 6H_2O$] mixed 2:1 with seawater; modified after Messenger *et al.* 1985) for 30–45 min. The body was then removed from the shell by cutting the two retractor muscles which attach the body to the shell; thereafter, the animal was sacrificed by decapitation. The anterior part of the hood, the tentacles, the funnel and the buccal mass were removed. The remaining head tissue was split mid-sagittally into two halves and each half was mounted median side up in a preparation dish filled with cold seawater. The dissection was done under a stereomicroscope (Wild M5) and with fibre optic illumination. The slightly yellow nerve tissue of the supra- and sub-oesophageal brain cords and its surrounding white connective tissue were carefully removed in layers (using a pair of fine forceps, spring scissors and razor blade splinters) until the statocyst was seen (for the anatomy of the nervous system of *Nautilus*, see Young 1965). With proper illumination, the lucent white mass of statoconia inside the statocyst cavity could easily be distinguished from the yellowish nerve and any other tissues. For subsequent dissection, the cut-out statocyst was transferred into a smaller dish coated with black wax.

For LM and TEM, four statocysts were used. To open a statocyst, a small hole was cut into its wall with a razor blade splinter, allowing the statoconia mass to drain out. The statocyst wall was then cut sagittally into two halves. Any remaining statoconia in the statocyst cavity were carefully washed out with a gentle stream of seawater from a 1 ml syringe. After fixation in 2% OsO_4 (Zetterquist buffer; pH 7.4) for 1.5 h at 4 °C, the two statocysts halves were cut into smaller pieces, dehydrated in graded ethanol solutions, and embedded in Epon. For LM, serial semi-thin sections (3–5 μm) were cut with a glass knife on a LKB 8800 Ultratome III microtome, and analysed and photographed with a Leitz Orthoplan transmission bright field photomicroscope. For TEM, ultrathin sections (70–80 nm) were cut with a Diatome diamond knife on a LKB 8800 Ultratome III microtome and viewed with a JEOL 100 C/X transmission electron microscope.

For SEM, six statocysts were used. They were dissected and cut into pieces as described above. Fixation was either in 2% OsO_4 (Zetterquist buffer;

pH 7.4) for 1.5 h at 4 °C; or in 4% glutaraldehyde (isotonic phosphate buffer; pH 7.3) for 2 h at 4 °C; or in 2.5% glutaraldehyde for 2 h, postfixed in 1% OsO_4 for 1 h, treated with saturated thiocarbohydrazide solution for 10 min, and again fixed in 1% OsO_4 for 1 h (isotonic phosphate buffer; pH 7.3; OTO-Method, see Murphy 1978). Thereafter, the tissue was dehydrated in graded ethanol solutions, critical point dried in a Balzers CPD 020 unit, gold–palladium coated with a Hummer II sputter unit (Technics, Alexandria, Virginia, USA), and viewed with a scanning electron microscope (Topcon DS-130-Dual Stage, Pleasanton, California, USA).

(*c*) *Statocyst operation on living Nautilus*

One animal was used for a statocyst operation. It was anaesthetized with a magnesium chloride solution (7.5% magnesium chloride [$MgCl_2 \times 6H_2O$] mixed 2:1 with seawater; modified after Messenger *et al.* 1985). When muscle movements ceased (after 20–30 min), the animal was transferred into a plastic dish (20 cm × 30 cm × 15 cm) filled with anesthetic solution. The bottom of the dish was covered with rigid foam plastic, cut out to fit the animal's shell. The animal was placed on its lateral side and secured in position in the foam mould with long plastic pins. The exposed eye was carefully bent dorsally with a small hook to uncover the olfactory tentacle. The subsequent procedures were done under stereomicroscopical control. To expose the statocyst, an incision was made ventrally to the eye where the mantle is attached to the head. With a razor blade splinter a window (5 mm long; 5 mm high; 5 mm deep) was cut into the cartilage ventral to the olfactory tentacle and in slightly posterior direction until the coelomic cavity was opened. Care was taken not to cut into the blood sinus that is present ventro-laterally of the statocyst. The statocyst could be easily identified by its lucent white statoconial mass and was then removed with a pair of forceps; remaining statocyst fragments were removed with a pipette. After operation, the animal was placed in, and the gills flushed with, cool oxygen-saturated seawater. Recovery was within 30 min.

(*d*) *Behavioural experiments*

To measure funnel movements in response to dynamic rotatory stimulation, five animals were used. Stimulation was sinusoidal oscillations of the animal around its vertical body axis. Almost all experiments were done with an oscillation frequency of 0.03 Hz and a peak velocity of 135° s^{-1} (peak acceleration 25° s^{-2}) because these stimulation conditions caused very clear funnel responses. One cycle of oscillation is defined as accelerating in one direction from zero to peak velocity and decelerating back to zero, then change of direction and accelerating again to peak velocity and decelerating back to zero. Positive values indicate counterclockwise (ccw) and negative values clockwise (cw) stimulus directions. In addition,

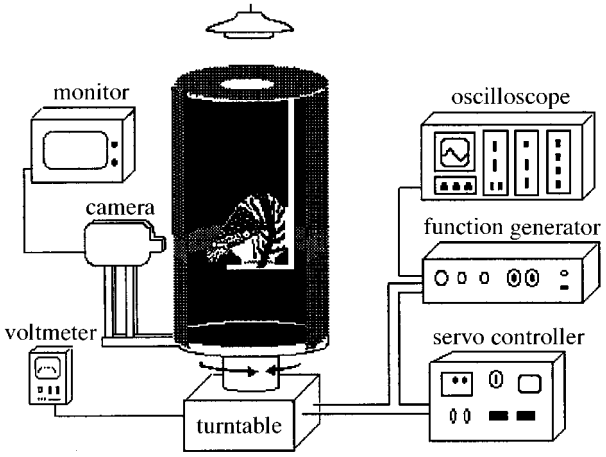

Figure 1. Experimental set-up to oscillate restrained *Nautilus* around its vertical body axis; visual cues are excluded by a black screen around the circular tank. The animal was filmed from anterior with a camera fixed to the turntable (except in the experiments in which the animal was stationary in an oscillating tank).

optokinetic experiments were performed with the animal stationary, and experiments with combined statocyst and optokinetic stimulations. A single experimental trial consisted of at least one complete cycle of oscillation. In general, all experimental trials were continued as long as the animals showed good responses, but every 15 min a break of 15 min was given to aerate and cool the seawater; also food was given to keep the animal alert.

(*e*) *Experimental set-up*

The experimental set-up allowed passive rotations of an animal around a vertical body axis, i.e. in the horizontal plane. The set-up consisted of an animal holder and a cylindrical plexiglas aquarium (inner diameter 27 cm; height 43 cm) mounted on a turntable (figure 1). The turntable was connected to a torque motor (23 lb-ft DC torque motor, Inland Corp.) that was controlled by a velocity servo-driven function generator (Wavetec 30 MHz, Model 162) to allow changes of frequency and velocity of oscillation. The animal was placed in the seawater-filled aquarium and fixed with a rubber band to a foam plastic mold of an animal holder (figure 1). The holder kept the animal in its normal upright position and was attached to the aquarium lid such that it allowed one to centre the animal in the axis of rotation (i.e. with the axis between the animal's left and right eye). For some experiments, the holder was fixed to a fibreglass device above, and separate from, the aquarium; this allowed rotation of the aquarium around a stationary animal. During the experiments with statocyst stimulation possible visual cues for rotation were excluded with a black screen surrounding the aquarium. To perform optokinetic and combined statocyst–optokinetic stimulations, the black screen was replaced by a black and white striped cylinder (diameter 28 cm; spatial wavelength $\lambda = 22.5°$; eight black and eight white stripes, each 5.46 cm wide and

PHILOSOPHICAL TRANSACTIONS OF THE ROYAL SOCIETY B BIOLOGICAL SCIENCES

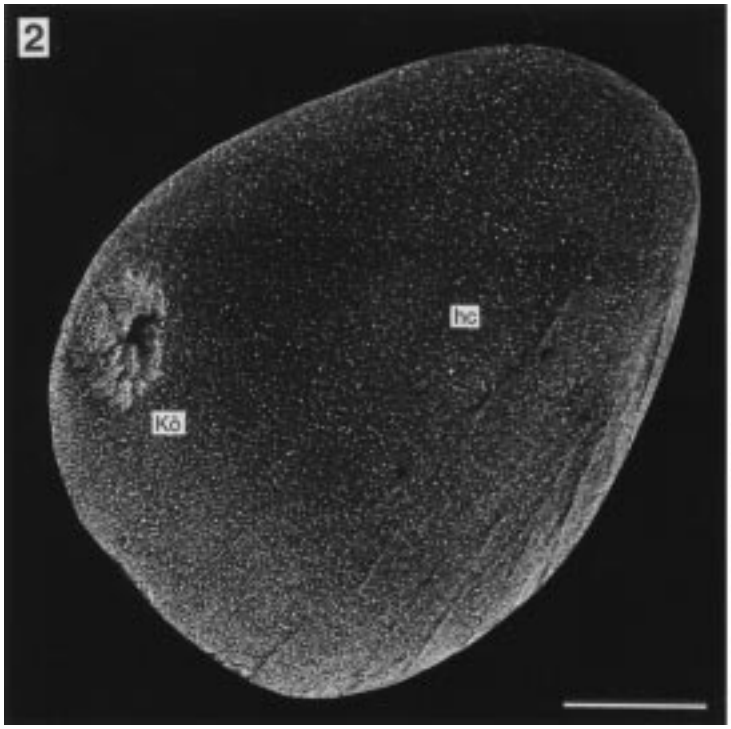

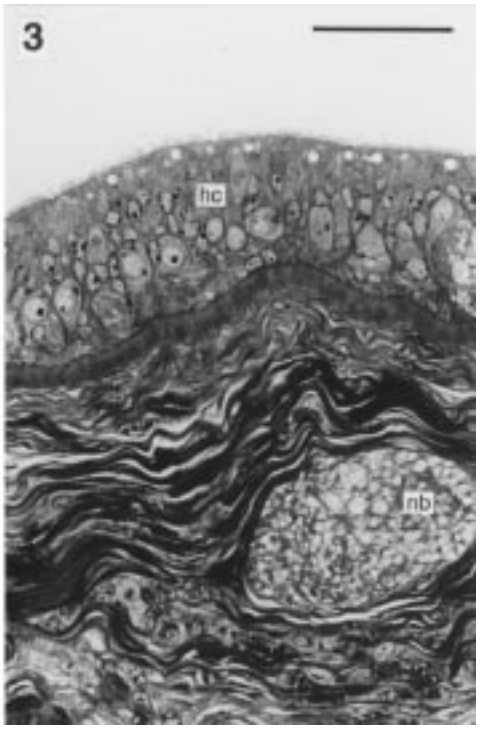

Figure 2. Statocyst of *Nautilus* sagittally cut and viewed from medial to show its oval shape; the statoconia are removed. At gross morphological level no separation into a gravity and an angular acceleration receptor system is evident; instead, the entire inner wall is lined with 130 000–150 000 hair cells (hc). The Kölliker's canal (Kö) opens laterally and connects the statocyst lumen with the exterior. SEM. Scale bar 500 μm.

Figure 3. Sensory epithelium of the statocyst, comprising hair cells (hc) and supporting cells. A nerve bundle (nb) is seen underneath the epithelium. LM (transverse section). Scale bar 50 μm.

40 cm high). A circular fluorescent light bulb (about 6 lux at the position of the animal) was centred above the aquarium. During all experiments, a black curtain surrounded the entire set-up.

(*f*) *Recording and analysis*

The anterior view of the animal was recorded with a CCD camcorder (Sony Handycam Hi8) through a narrow circular window in the screen surrounding the aquarium (figure 1). The camera was mounted to the turntable, i.e. was oscillated in synchrony with the animal. When the animal was stationary (i.e. when the aquarium was rotated around the animal), the camera was fixed on a tripod in front of the aquarium and separate from the turntable; in that case, the photographic recording was done through a narrow, horizontal slit in the screen all around the aquarium. On-line observation of the animal inside the aquarium was possible by a video monitor connected to the camera. A digital time code (1 s resolution) was included into the video picture, as well as the reading of a voltmeter connected to the DC output of the turntable motor tachometer; the latter provided information about the start and stop of stimulation in each trial and thus allowed one to synchronize the measurements. For optokinetic and combined statocyst–optokinetic stimulations, the black and white striped cylinder was partly included in the video picture to provide information about stimulus direction, start and stop.

For analysis of the recordings, a video recorder (Sony EV-S900 NTSC) was used that allowed bidirectional single frame transport and display of video still pictures. Single frame analysis was done with a computer supported video analysis system, consisting initially of a Macintosh Quadra 900 computer with a video capture card (later of a Macintosh Power PC AV 8100) and a public domain software program (NIH Image 1.52). This allowed measurements of the funnel positions as seen on the computer monitor with respect to an internal reference. The funnel position was determined by the x-coordinate of the most dorsal part of the funnel aperture. The data were then transformed into movements by similar morphometric measurements of the 'real' animal and the computer image. The distance between the far-most right and far-most left x-coordinates represents approximately a chord on the circle of rotation of the funnel. For all animals, the radius of that circle was 30 mm. The linear data were transformed into angular data ($\sin^{-1}(x/r)$). These, however, are relative values representing only a portion of the actual funnel movements when seen from above (the experimental set-up did not allow such video recordings); the maximum 'real' horizontal funnel deviation is estimated to be 90° in either direction. The middle position (x) of the funnel was defined according to the mid-sagittal plane of the animal (see also figures 24 and 27). Based on the known amplitude and frequency of the motor output, the stimulus velocity

PHILOSOPHICAL TRANSACTIONS OF THE ROYAL SOCIETY B BIOLOGICAL SCIENCES

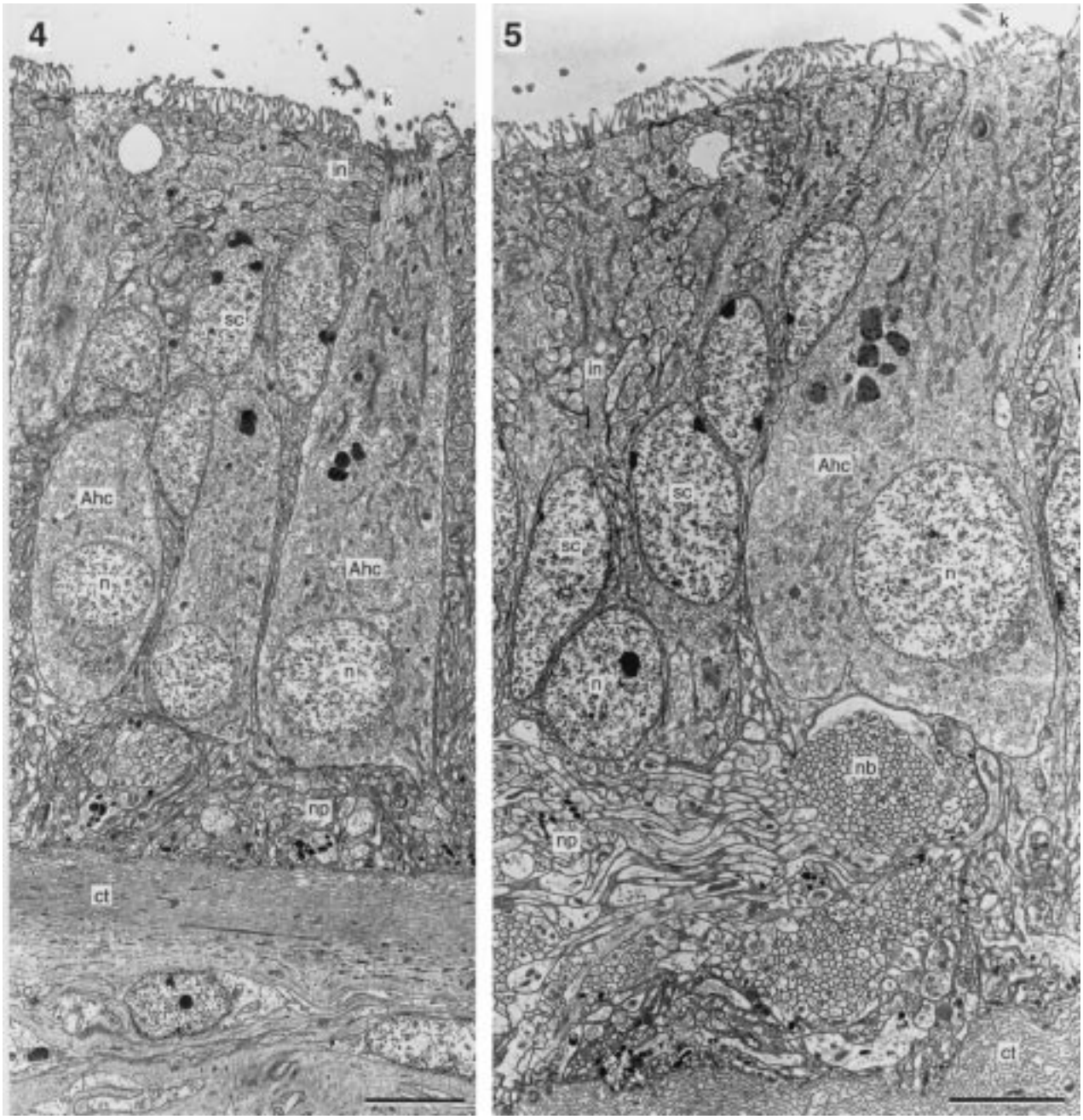

Figure 4. Sensory epithelium of the ventral half of the statocyst, showing type *A* hair cells (Ahc) and supporting cells (sc). Note interdigitations (in) between the apical membranes of the supporting cells. ct, connective tissue; k, kinocilia; n, nucleus, np, nerve plexus. TEM (transverse section). Scale bar 5 µm.

Figure 5. Sensory epithelium of the ventral half of the statocyst, showing type *A* hair cells (Ahc) and supporting cells (sc). Nerve bundles (nb) and a nerve plexus (np) are seen underneath the epithelium. Note the heavy interdigitations (in) between the apical membranes of the supporting cells. ct, connective tissue; k, kinocilia; n, nucleus. TEM (transverse section). Scale bar 5 µm.

curves (and the stimulus acceleration curve in figure 24) were calculated and synchronized with start and stop of stimulation, as indicated by the voltmeter reading.

(*g*) *Database*

Recordings from five animals were used for data analysis. Every 10th, 15th, 20th, 30th and 40th video frame was captured for measurement and data collection. In figure 29, funnel movement is plotted before and during the start of the stimulus to show that the initial acceleration step did not affect the funnel movements; in all other figures, the first cycles of oscillation were not included in the analysis.

3. RESULTS

(*a*) *Anatomy of the statocyst*

The two statocysts of *Nautilus* are located ventrolaterally on either side of the brain; they are embed-

PHILOSOPHICAL TRANSACTIONS OF THE ROYAL SOCIETY B BIOLOGICAL SCIENCES

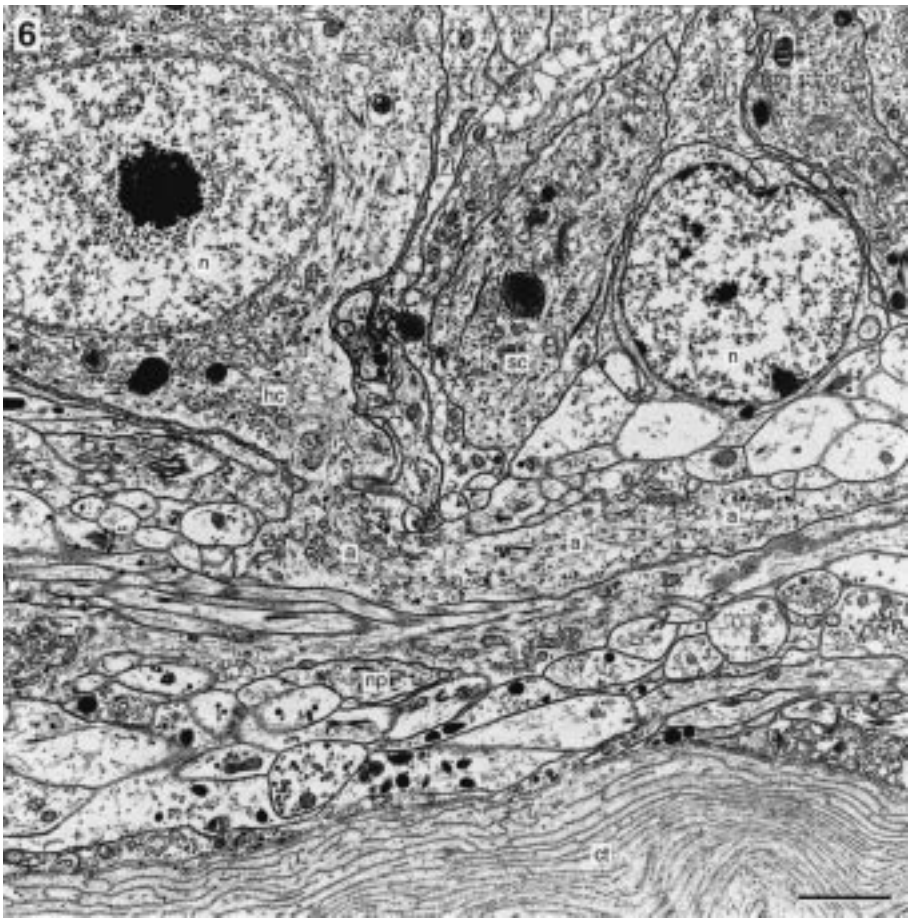

Figure 6. Primary sensory hair cell (hc) with an axon (a) leaving its base; the axon enters the nerve plexus (np) underneath the epithelium. ct, connective tissue; n, nucleus; sc, supporting cell. TEM (transverse section). Scale bar 2 μm.

ded in fibrous tissue where the three main brain cords meet (Young 1965). In the adult animal, the left and right statocyst are about 20 mm apart. Each statocyst is of ovoid form (2 mm × 2.5 mm; figure 2) and is oriented such that its long axis is transversally and approximately at 45° to the horizontal plane of the animal, with its lateral end higher than the medial (Young 1965). The inner surface of a statocyst measures approximately 15 mm^2 and is lined throughout with epithelial cells. The lumen of the statocyst measures approximately 6 mm^3; its lower half is filled with a large number of small free-moving calcareous statoconia and its upper half with endolymph.

(i) *Statocyst epithelium*

The epithelium of the statocyst comprizes a single layer of columnar epithelial cells (figures 3–5). It consists of four different types of cells: Type *A* and type *B* receptor hair cells, supporting cells and the ciliated cells of the opening of the Kölliker's canal. A nerve plexus is present underneath the epithelium; it separates the epithelial cells from the statocyst wall which consists of a thick layer of connective tissue (figures 4–6).

Type *A* and type *B* receptor hair cells have the same cone-like shape, with a small surface area and a larger base (height about 38 μm; width apically about 4 μm, basally about 12 μm). The nucleus is spherical and located in the proximal part of the cell; it contains a large electron-dense nucleolus usually in, or close to, the centre of the nucleus (figure 6). No obvious basal lamina was seen underneath the epithelial cells. From the apical surface of the hair cells kinocilia (with an internal $9 \times 2 + 2$ tubuli content) and microvilli project into the lumen of the statocyst. The hair cells do not carry stereovilli (stereocilia). From the basal body of each kinocilium numerous well developed rootlets originate and radiate down into the cell; the rootlets are cross striated with a periodicity of 0.05 μm (figure 7). About 0.3 μm above the hair cell surface, the kinocilia and microvilli are embedded in a layer of extracellular material that is about 1 μm thick and reaches to the tips of the microvilli (figure 8).

Each hair cell is surrounded by several supporting cells of irregular shape (figures 4–6; see also figure 17). Hair cells and supporting cells are connected by desmosomes (compare figure 17). Neighbouring supporting cells show many well developed interdigitations along their apical membranes (figures 4 and 5; see also figure 16). At their apical surface, the supporting cells bear microvilli of the same length as those of the hair cells (figure 8). The nucleus of the supporting cells is ovoid with electron-dense chromatin usually seen at its periphery (figure 4; see also figure 19).

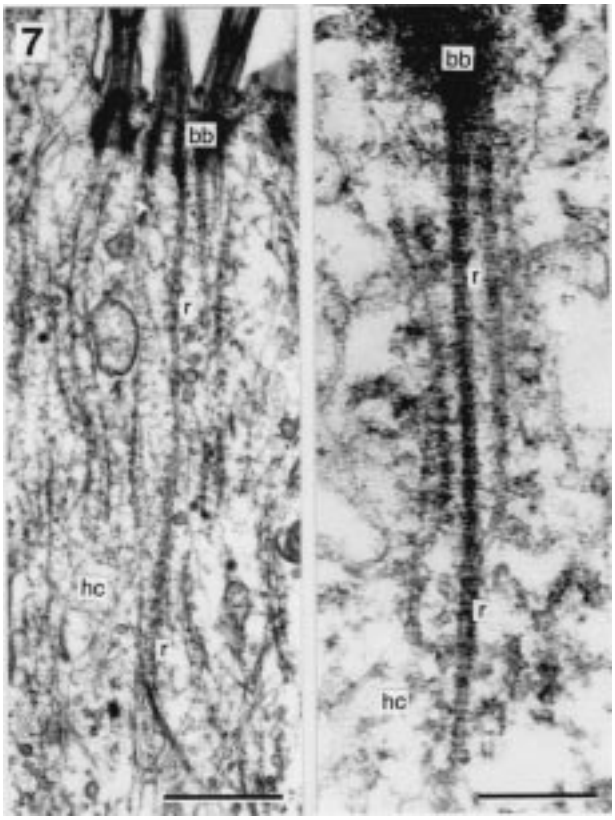

Figure 7. Well-developed rootlets (r) arise from the basal bodies (bb) of the kinocilia of the hair cells (hc) and run straight down into the cell soma. TEM (transverse section). Scale bars 1 μm (left) and 0.2 μm (right).

(ii) *Arrangement of receptor hair cells*

There is a total of 130 000–150 000 receptor hair cells in each statocyst; they are regularly distributed over its inner surface, excluding the area around the opening of the Kölliker's canal (figures 2 and 9). Based on the arrangement and length of their kinocilia, two morphologically different types of receptor hair cells can be distinguished: type *A* hair cells in the ventral half of the statocyst, and type *B* hair cells in its dorsal half (figure 9). A distinct borderline is seen at the equator of the statocyst where the two hair cell types meet.

Type *A* hair cells carry 10–15 kinocilia; they are 4–5 μm long and are arranged in a single row (figures 10 and 11). The length of the long axis of the row varies between 2 and 4 μm. The row is not centred on the cell surface but is placed peripherally (figures 10 and 11); this asymmetric position is the same in neighbouring type *A* hair cells (figures 10 and 11). In addition to kinocilia, type *A* hair cells carry microvilli (length 1.25 μm); the ones closest to the kinocilia are regularly spaced right beside and along the kinociliary row (figure 14). The long axes of the ciliary rows of neighbouring type *A* hair cells are oriented parallel to each other (figures 10 and 11). Close to the equator of the statocyst, these long axes are oriented horizontally.

Type *B* hair cells carry 8–10 kinocilia. As in type *A* hair cells, they are all placed peripherally on the cell surface, although not in a row but irregularly arranged (figures 12 and 13). The cilia are 7–10 μm long and thus are twice as long as those of type *A* hair cells. In some type *B* hair cells, the kinociliary arrangement seems circular or ellipsoid (figures 12 and 13). The microvilli of type *B* hair cells have the same length (1.25 μm) as those of type *A* hair cells but are more numerous (figure 17).

(iii) *Morphological polarization of the receptor hair cells*

Type *A* and type *B* hair cells are both morphologically polarized according to several criteria: (1) the orientation of the internal $9 \times 2 + 2$ tubuli of their kinocilia (figure 14); (2) the orientation of the basal feet that are attached to the basal bodies of the kinocilia (figures 15–17); (3) the peripheral location of the kinocilia on the cell surface (figures 11 and 12); and (4) in type *A* hair cells only, the inclined position of the ciliary group relative to the surface of the cell and epithelium (figure 10). The position of the basal foot relative to the cell defines and indicates the cell's direction of morphological polarization. For all kinocilia of a given type *A* or type *B* hair cell these directions are the same and consequently polarize a hair cell into one direction. This direction is also at right angles to the connecting line between the two central tubuli of the kinocilium and, associated with the peripheral position of the kinocilia, toward the centre of the apical cell surface; in type *A* hair cells it is at right angles to the long axis of the kinociliary row (figures 14 and 15) and opposite to the acute angle the ciliary row forms with the cell surface. Such morphological polarization is well known in cephalopod and vertebrate mechanoreceptive hair cells; it correlates with a physiological polarization (Budelmann & Williamson 1994).

(iv) *Innervation of the receptor hair cells and the statocyst nerve*

An axon arises from the base of type *A* and type *B* hair cells and joins the nerve plexus underneath the epithelium (figures 4 and 6). The presence of an axon classifies the hair cells as primary sensory cells. Axons of several hair cells form small bundles; these join and form larger bundles (figures 3, 5, 18 and 19) which finally constitute the statocyst nerve. The diameters of individual fibres range from 0.3–1.5 μm. The nerve leaves the statocyst medio-dorsally and enters the brain at the level of the magnocellular lobe (Young 1965). The nerve plexus underneath the hair cell epithelium includes a number of profiles that are filled with round clear, or electron-dense, synaptic vesicles (figures 20 and 21). The profiles, most likely, are part of an efferent innervation of the hair cells.

(v) *Kölliker's canal*

The statocyst cavity communicates with the exterior by the Kölliker's canal. Leaving the statocyst, it proceeds laterally towards the body surface and opens via a small pore ventral to the olfactory tentacle below the eye (Young 1965). The inner surface of the canal is covered with ciliated cells (Young 1965). Also, the area around the opening of the canal into

PHILOSOPHICAL TRANSACTIONS OF THE ROYAL SOCIETY B BIOLOGICAL SCIENCES

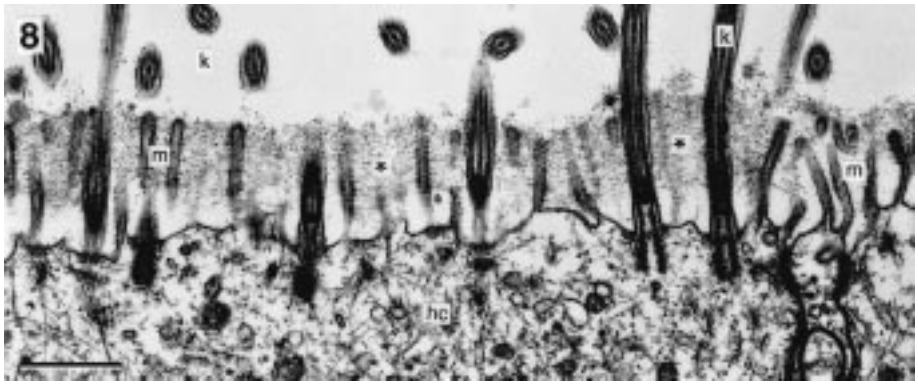

Figure 8. Apical part of a hair cell (hc) showing kinocilia (k) and microvilli (m). Note the extracellular electron-dense material (asterisk) that connects the kinocilia and microvilli. TEM (transverse section). Scale bar 1 μm.

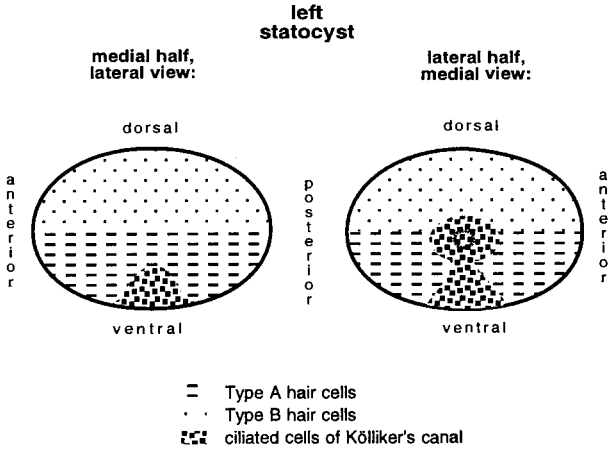

Figure 9. Diagram of the medial (left) and lateral (right) half of the statocyst, showing the distribution of type *A* and type *B* hair cells and the ciliated cells of the Kölliker's canal.

the statocyst cavity and an area ventral to the opening is densely covered with ciliated cells (figures 9 and 22). Each ciliated cell bears 30–50 irregularly arranged kinocilia; they are 10–12 μm long and thus longer than those of type *A* and type *B* hair cells.

(vi) *Possible functions of the statocyst*

The statocyst contains a freely moving mass of numerous small calcareous statoconia, as well as endolymph. Most statoconia are of ovoid form but some are spherical (figures 13 and 23). They range in length from 1.7–17 μm; sometimes two or more statoconia are fused and form a cross (figure 23; see also Morris 1989). There is no sign of mucous or any other material that mechanically connects the statoconia to each other or to the cilia of the hair cells. Because the specific weight of the statoconia is higher than that of the endolymph (Lowenstam *et al.* 1984), in an upright position of the animal the statoconia fill the lower (ventral) half of the statocyst, which is lined with type *A* hair cells; in that same position, type *B* hair cells, which line the upper (dorsal) half of the statocyst, are in contact with the endolymph. The separation of the two hair cell types within the statocyst and the fact that polarization is not essential for gravity reception in statocysts with free-moving statoconia (or statoliths) suggests that the *Nautilus* statocyst is sensitive to angular accelerations besides its function as a gravity receptor organ (see Discussion). To date, however, no such experimental data are available that indicate that *Nautilus* is able to sense angular accelerations. Consequently, experiments were designed that allowed measurements and analyses of possible compensatory funnel responses of *Nautilus* to angular accelerations on a horizontal turntable, i.e. without changes in position of the animal relative to the direction of gravity.

(*b*) *Behaviour*

To test for sensitivity to angular accelerations, behavioural experiments were performed to investigate motor responses of the funnel of restrained *Nautilus* exposed to dynamic sinusoidal oscillations around a vertical (yaw) body axis. The funnel (hyponome) is a mobile muscular tube located antero-ventrally of the head; it is used to direct the water that is expelled out of the mantle cavity. During jetting the animal moves in a direction opposite to the direction towards which the funnel points.

Although angular acceleration was the stimulus during sinusoidal oscillation, velocity as a parameter of the stimulus is plotted in the figures because the funnel response has dynamic properties that are related to stimulus velocity. In figure 24, stimulus acceleration is also plotted to show its relationship to stimulus velocity (stimulus acceleration phase-leads stimulus velocity by 90°) and funnel position.

(i) *Sinusoidal oscillations of Nautilus*

Sinusoidal oscillations (frequency 0.03 Hz, peak velocity 135° s^{-1}, peak acceleration 25° s^{-2}) of restrained animals around a vertical body axis elicit two different funnel responses: (i) a compensatory funnel response, i.e. the funnel moves in the same direction as the direction of the stimulus, thus jetting would move the animal in a direction opposite to that of the stimulus; and (ii) a funnel follow response, i.e. the funnel moves in a direction opposite to that of the stimulus, thus jetting would move the animal in

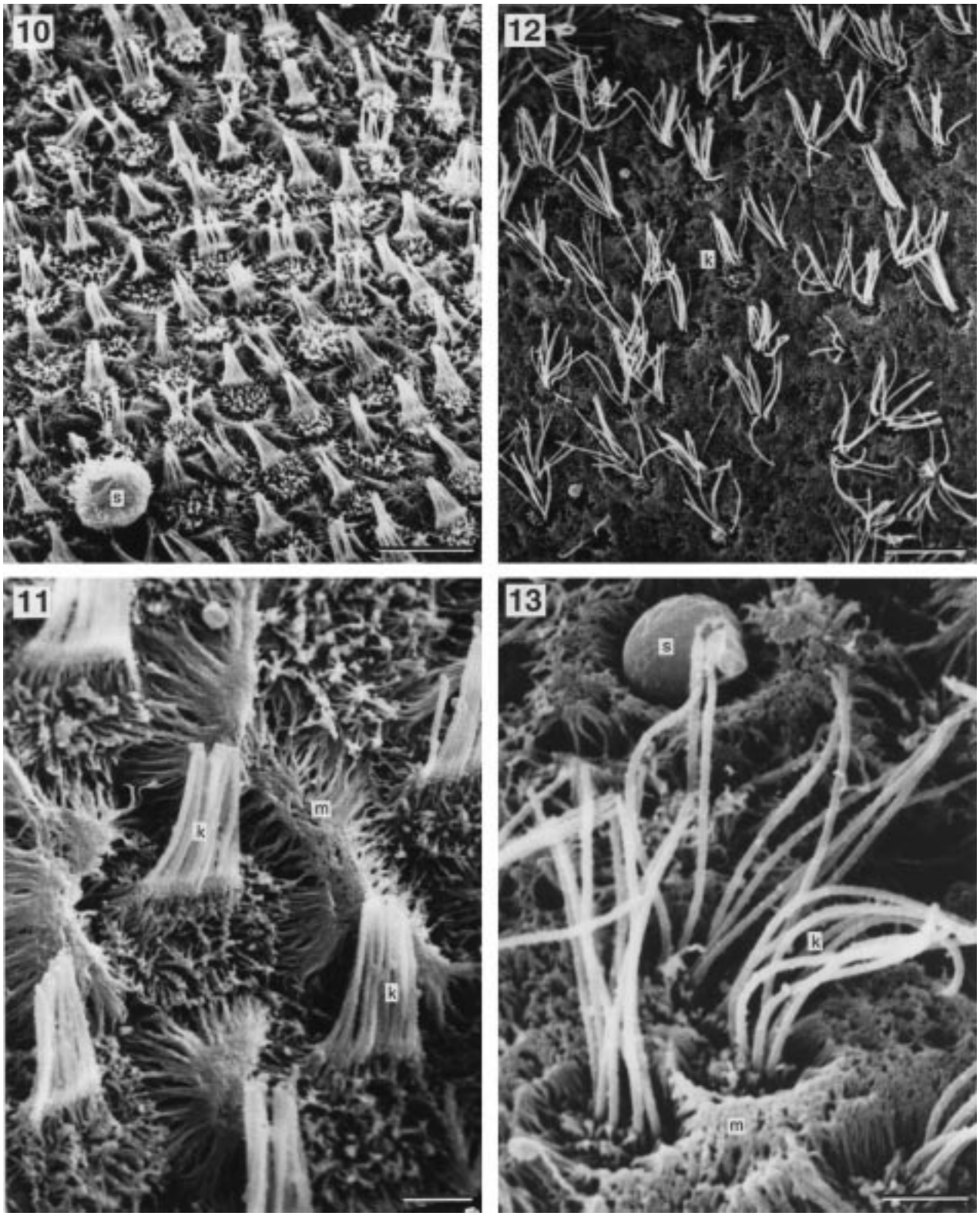

Figure 10. Type *A* hair cells in the ventral half of the statocyst. Note the asymmetric position of the kinocilia on the circular surface of the hair cells. s, statoconium. SEM. Scale bar 10 µm.

Figure 11. Kinocilia (k) of type *A* hair cells arranged in rows on the cell surface. An individual type *A* hair cell carries 10–14 kinocilia arranged in an elongated row. Note the asymmetric position of the kinocilia on the cell surface. m, microvilli. SEM. Scale bar 2 µm.

Figure 12. Type *B* hair cells in the dorsal half of the statocyst. Note the asymmetric position of the kinocilia (k) on the circular surface of the hair cells. SEM. Scale bar 10 µm.

Figure 13. Kinocilia (k) of type *B* hair cells. An individual type *B* hair cell carries 8–10 kinocilia irregularly arranged on the cell surface. Note the asymmetric position of the kinocilia on the cell surface. m, microvilli; s, statoconium. SEM. Scale bar 2 µm.

PHILOSOPHICAL TRANSACTIONS OF THE ROYAL SOCIETY B BIOLOGICAL SCIENCES

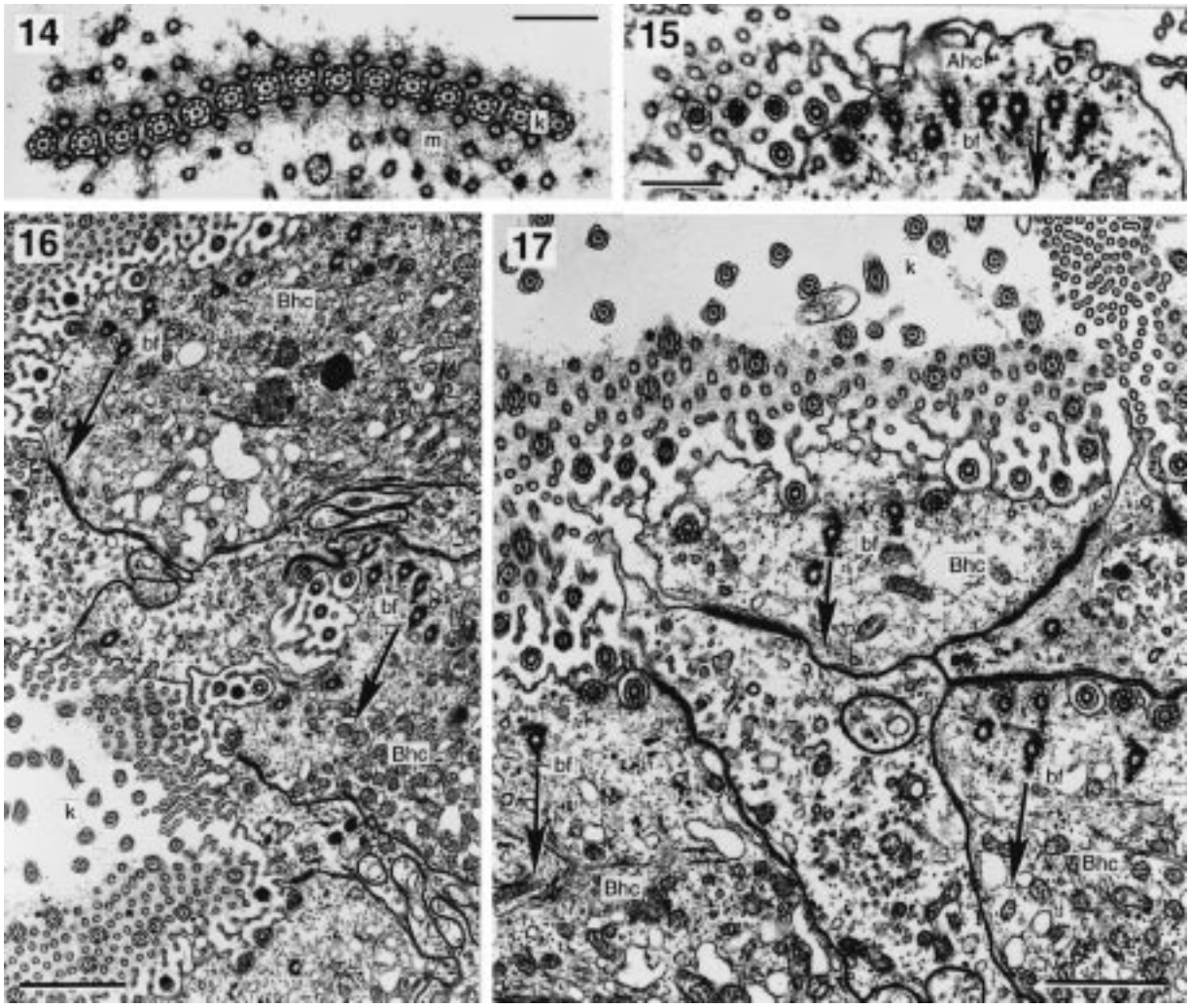

Figure 14. Cross section of a kinociliary row of a single type *A* hair cell. k, kinocilia; m, microvilli. TEM. Scale bar 1 μm.

Figure 15. Tangential section through the apical part of a type *A* hair cell (Ahc) at the level of the basal feet (bf). According to their orientation, all kinocilia are polarized in the same direction (arrow), which is at right angles to the long axis of the kinociliary row. TEM. Scale bar 1 μm.

Figures 16 and 17. Tangential sections at different magnifications through the apical part of type *B* hair cells (Bhc) at the level of the basal feet (bf). According to their orientation, all kinocilia (k) of individual hair cells, and of neighbouuring hair cells, are polarized in the same direction (arrows). Note the interdigitations between the membranes of supporting cells. TEM. Scale bars 2 μm (figure 22) and 1 μm (figure 23).

the same direction as that of the stimulus. In some cases the animals switched from one response to the other.

Compensatory funnel response. In figure 24, funnel positions of three animals are averaged during three oscillations and plotted together with stimulus velocity and stimulus acceleration. During the compensatory funnel response, the funnel moves in a direction opposite to that of the passive movement of the water column (figure 25); therefore, the compensatory funnel response is an active funnel movement. The funnel position curve is periodic and nearly in phase with the stimulus velocity curve, i.e. funnel deviation is largest when stimulus velocity is highest. The funnel position maxima reach 17° (±3.6° s.e.m.) during the clockwise part and 15° (±7.9° s.e.m.) during the counterclockwise part of the oscillation cycle and occur shortly before the maxima of the stimulus velocity curve (figure 24). The funnel position curve is nearly 90° out of phase with the stimulus acceleration curve, i.e. funnel deviation is largest when stimulus acceleration is lowest. The slopes of the funnel position curve are steeper during stimulus acceleration than during stimulus deceleration. Largest variations (s.e.m.) occur during the clockwise part of the oscillation cycle. The reason for this asymmetry is unclear; it might be due to the anatomical asymmetry of the muscular funnel.

During five consecutive oscillations, the peak amplitudes (10°) of the funnel position curve declined slightly (figure 26) and their phase positions became increasingly phase lagged as compared to the stimulus velocity curve (about 25°). Some small plateaus of the funnel position curve occurred during the clockwise parts of the oscillation cycles; again, the reason for this asymmetry is unclear. There was no compen-

PHILOSOPHICAL TRANSACTIONS OF THE ROYAL SOCIETY B BIOLOGICAL SCIENCES

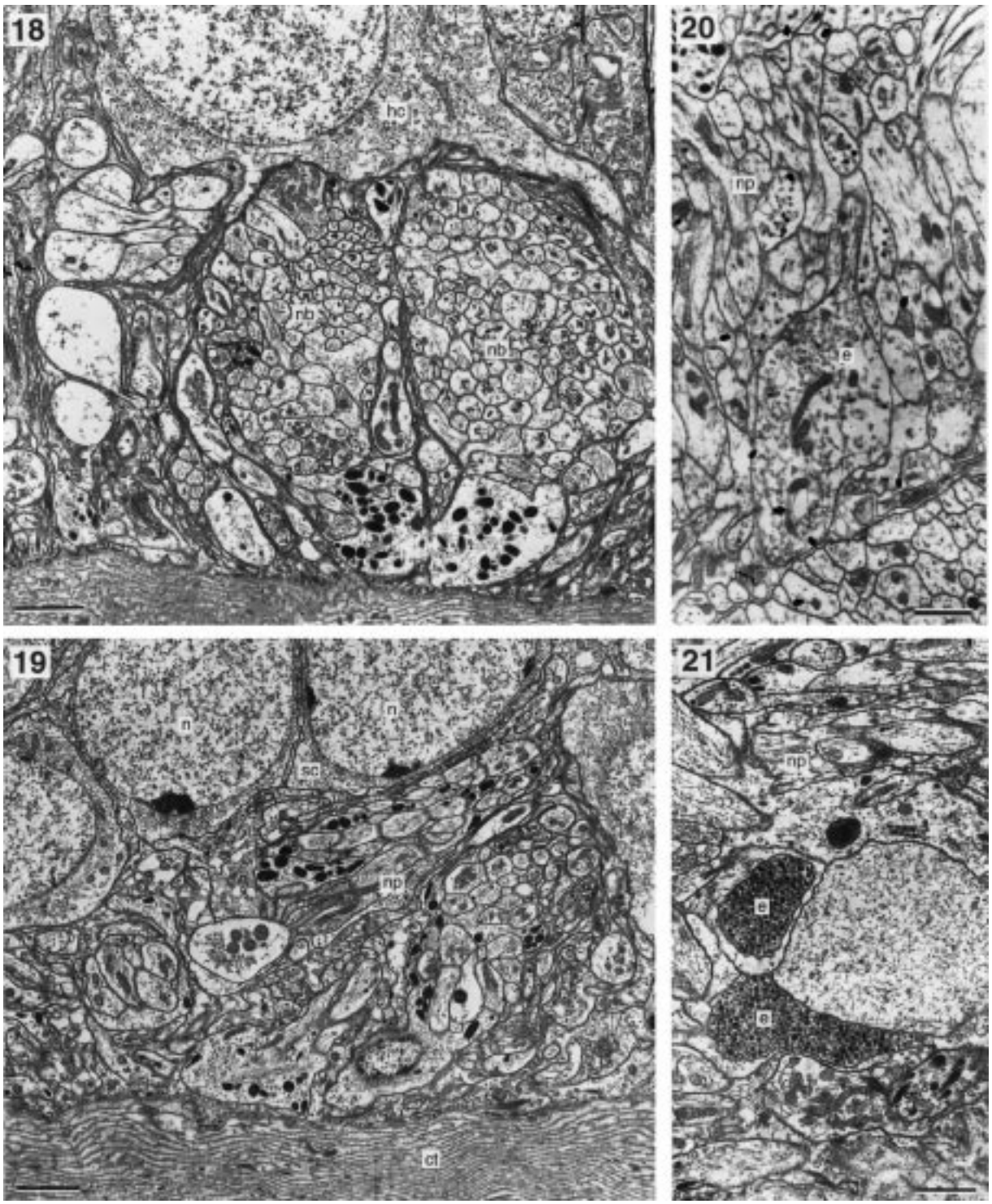

Figure 18. Nerve plexus with two nerve bundles (nb) underneath the hair cells (hc). TEM. Scale bar 2 μm.

Figure 19. Nerve plexus (np) underneath the hair cells, showing bases of supporting cells (sc) with large nuclei (n). Note the peripheral location of the nucleoli. ct, connective tissue. TEM. Scale bar 2 μm.

Figures 20 and 21. Sections through the nerve plexus (np) underneath the hair cells, showing efferent profiles (e) filled with clear (figure 20) and electron-dense (figure 21) synaptic vesicles. TEM. Scale bars 1 μm.

satory funnel response when the oscillation stopped.

Funnel follow response. In figure 27, funnel positions of three animals are averaged during three oscillations and plotted together with stimulus velocity against time. The funnel follow response is in a direction opposite to that of the stimulus, but in the same direction as that of the passive movement of the water column (figure 28). Therefore, it is difficult to decide whether the funnel follow response includes a component that is based on active funnel movements (see also Control experiments). The funnel position curve is periodic but almost 180° out of phase with the stimulus velocity curve (figure 27) and seems to have two distinct peaks (more obvious

PHILOSOPHICAL TRANSACTIONS OF THE ROYAL SOCIETY B BIOLOGICAL SCIENCES

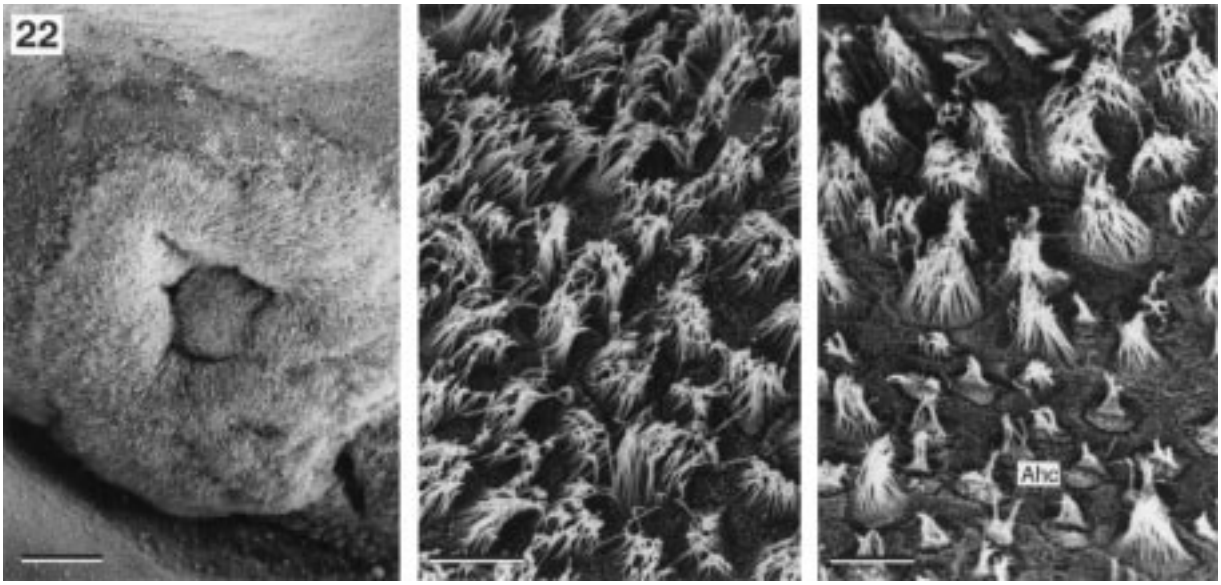

Figure 22. Kölliker's canal. Opening of the canal into the statocyst lumen (left), and ciliary bundles of the ciliated cells of the canal opening (middle) and in the transition area to type *A* hair cells (Ahc) in the ventral part of the statocyst (right). SEM. Scale bars 50 µm (left) and 10 µm (middle and right).

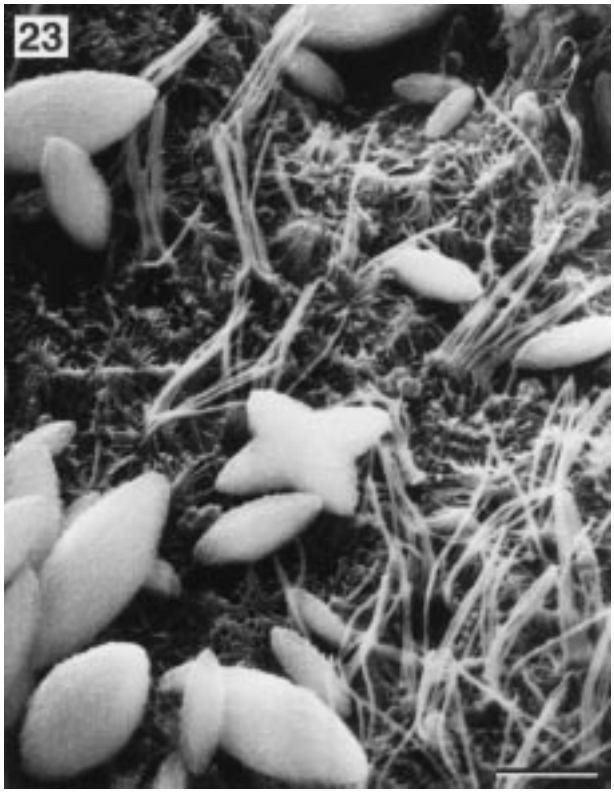

Figure 23. Individual ovoid- and cross-shaped statoconia; note their large variation in size. SEM. Scale bar 5 µm.

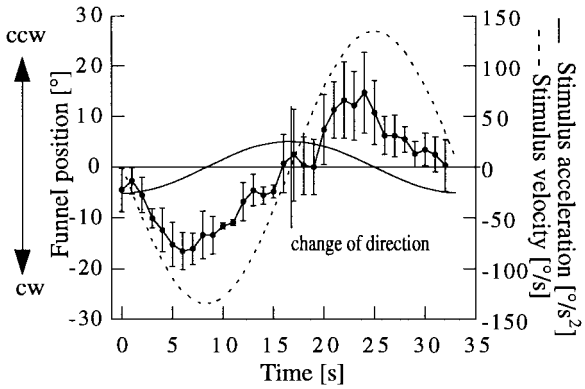

Figure 24. Compensatory funnel response of *Nautilus* during sinusoidal oscillation around a vertical body axis (dotted curve; right ordinate; frequency 0.03 Hz; peak velocity 135° s^{-1}). Funnel position (left ordinate) is superimposed on stimulus velocity (dotted curve and stimulus acceleration (solid curve; right ordinate, peak acceleration 25° s^{-2}). Averaged data of three animals during three oscillations (means ± s.e.m.). The funnel moves in the direction of the stimulus, i.e. jetting would move an unrestrained animal in opposite direction. Positive values indicate funnel position, stimulus velocity, and acceleration during the counterclockwise (ccw), and negative values during the clockwise (cw), part of the oscillation cycle.

during the counterclockwise part of the oscillation cycle). Maximum amplitude is 29° (±5.09° s.e.m.); this is higher than the maximum amplitude of the compensatory funnel response (compare figures 24 and 27). The slopes of the funnel position curve are the same during the acceleration and deceleration parts of the oscillation cycle.

During the first three of five consecutive sinusoidal oscillations, the peak amplitude of the funnel position curve was 33°, but then declined to below 20° (figure 29). In the same experiment, the funnel position curve of the funnel follow response showed small plateaus, which occurred during both the clockwise and the counter-clockwise parts of the oscillation cycles. As for the compensatory funnel response, during the five oscillations the phase position and amplitude of the funnel follow response changed slightly; the phase position became increasingly phase-lagged as compared to the stimulus velocity curve (figure 29; see also figure 26).

PHILOSOPHICAL TRANSACTIONS OF THE ROYAL SOCIETY B BIOLOGICAL SCIENCES

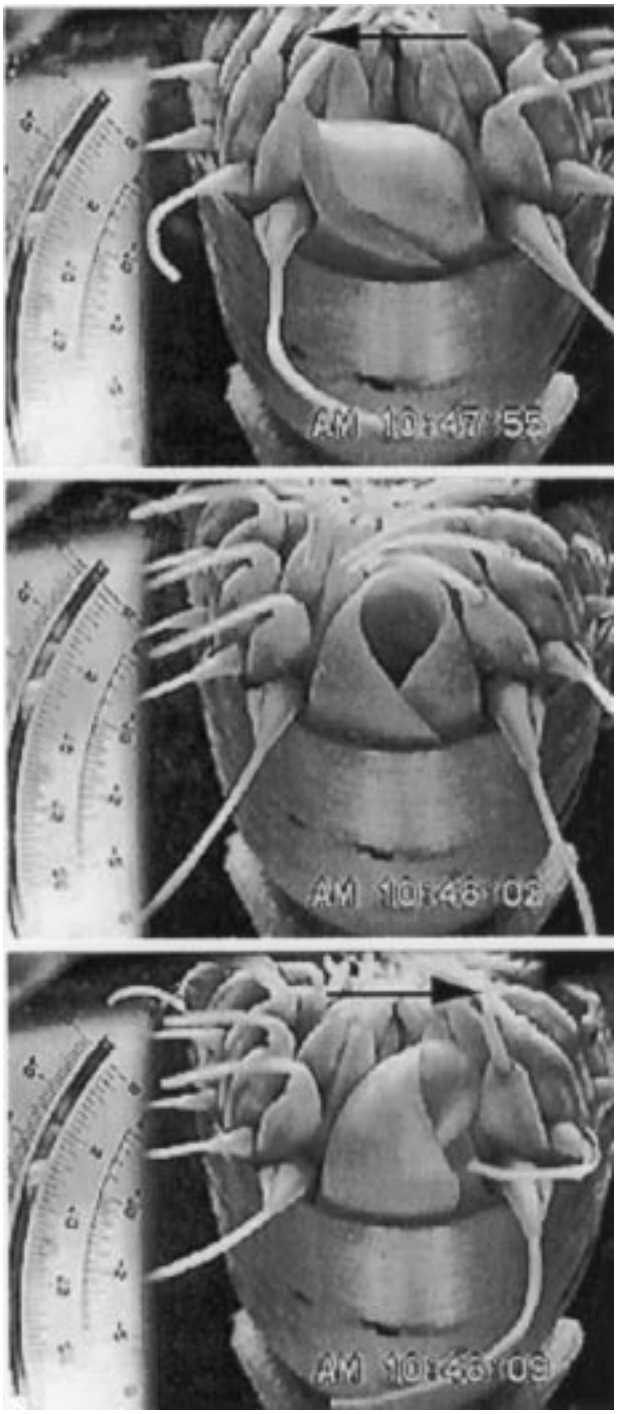

Figure 25. Video pictures of *Nautilus*, filmed from anterior, to analyse funnel position during sinusoidal oscillation around a vertical body axis. The voltmeter reading indicates stimulus velocity. The figures show compensatory funnel responses during one oscillation cycle. Arrows indicate direction of oscillation. Top: clockwise (cw) part of the oscillation cycle; middle: transition between clockwise and counterclockwise oscillation (= no oscillation) with the funnel in middle position; bottom: counterclockwise (ccw) part of the oscillation cycle. Note that the compensatory funnel response is in a direction opposite to the direction of the water movement (as indicated by the passive movement of the tentacles).

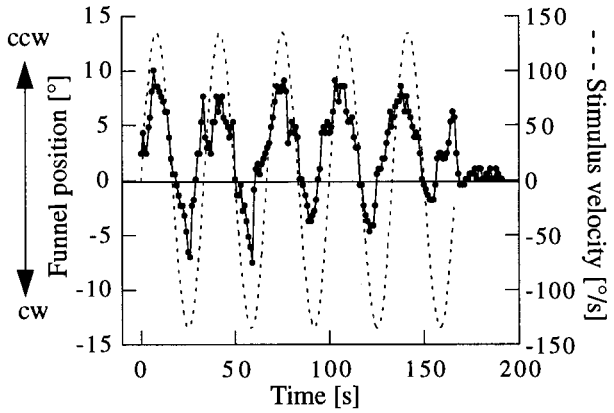

Figure 26. Compensatory funnel response of *Nautilus* during five sinusoidal oscillations around a vertical body axis (dotted curve; right ordinate; frequency 0.03 Hz; peak velocity 135° s^{-1}). The sequence represents five oscillations and 25 s after stop of stimulation (= end of the oscillation curve). One data point corresponds to one measurement.

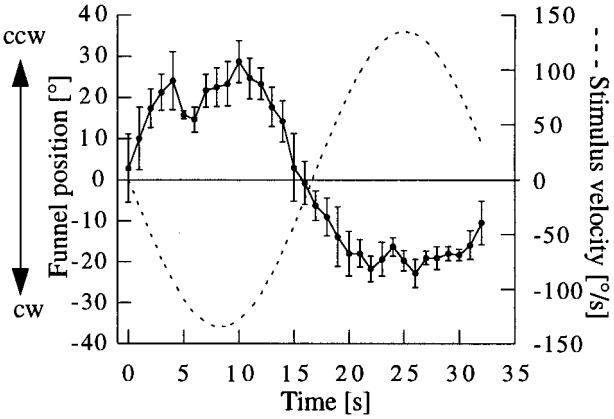

Figure 27. Funnel follow response of *Nautilus* during sinusoidal oscillation around a vertical body axis (dotted curve; right ordinate; frequency 0.03 Hz; peak velocity 135° s^{-1}). Averaged data of three animals during three oscillations (means ± s.e.m.). The funnel moves in a direction opposite to the direction of the stimulus, i.e. jetting would move an unrestrained animal in stimulus direction.

Changes between the two funnel responses. In all tested animals, the compensatory funnel response and the funnel follow response occurred at a ratio of about 1:1. In addition, some animals switched from one response to the other within a single experimental trial. In figure 30, the funnel positions of a single animal are plotted together with stimulus velocity against time during three oscillations. During the first one and a half oscillations the response is a compensatory funnel response with a peak amplitude of 14°. Then, with the beginning of the second part of the second oscillation cycle (after the change of stimulus direction), the response changed to a funnel follow response. During the second part of the third oscillation cycle the funnel follow response switched back to a compensatory response. The switch from one funnel response to the other was accompanied by a small decrease in amplitude (approximately 4°).

PHILOSOPHICAL TRANSACTIONS OF THE ROYAL SOCIETY B BIOLOGICAL SCIENCES

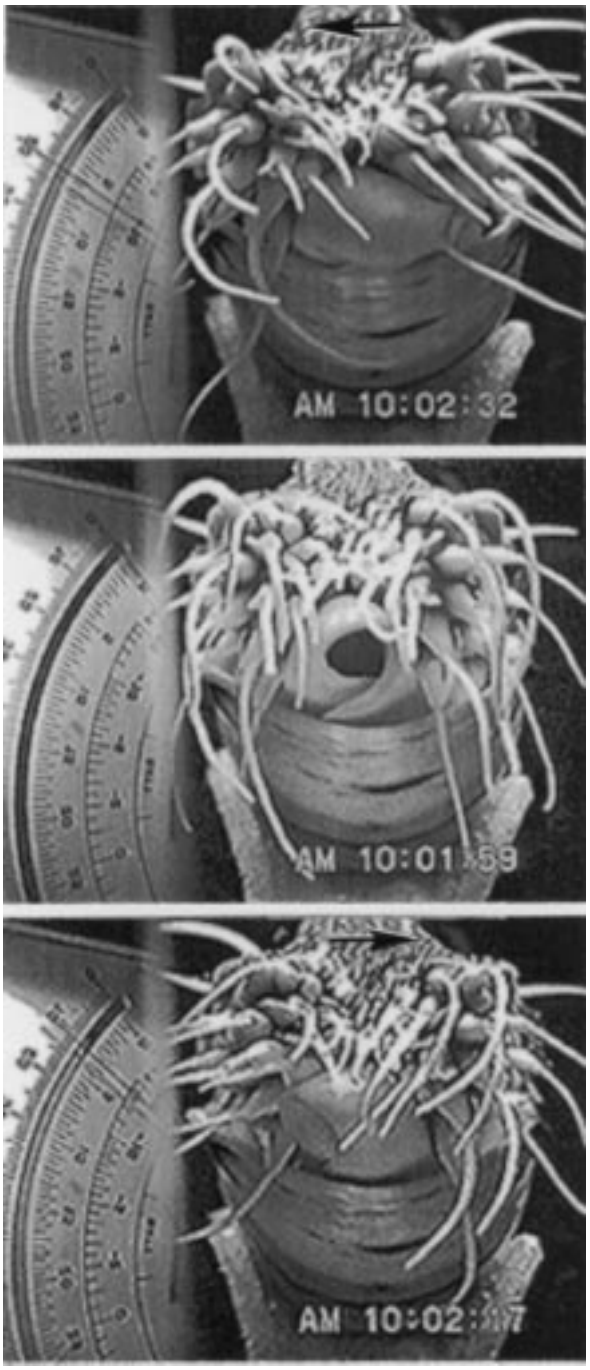

Figure 28. Video pictures of *Nautilus*, filmed from anterior to analyse funnel position during sinusoidal oscillation around a vertical body axis. The voltmeter reading indicates stimulus velocity. The figures show funnel follow responses during one oscillation cycle. Arrows indicate direction of oscillation. Top: clockwise (cw) part of the oscillation cycle; middle: transition between clockwise and counterclockwise oscillation (= no oscillation) with the funnel in middle position; bottom: counterclockwise (ccw) part of the oscillation cycle. Note that the funnel follow response is in the same direction as the water movement (as indicated by the passive movement of the tentacles).

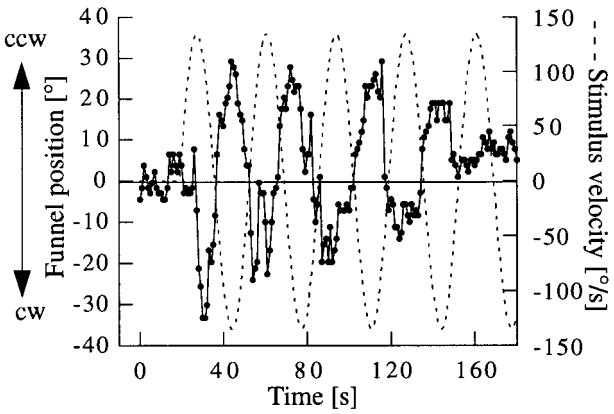

Figure 29. Funnel follow response of *Nautilus* during five sinusoidal oscillations around a vertical body axis (dotted curve; right ordinate; frequency 0.03 Hz; peak velocity 135° s^{-1}). One data point corresponds to one measurement.

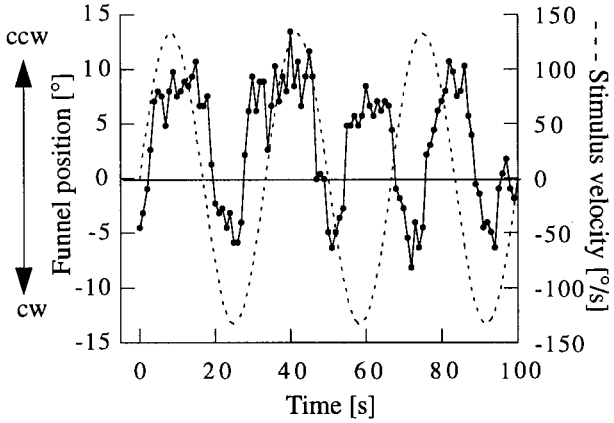

Figure 30. Compensatory funnel response and funnel follow response of *Nautilus* during three oscillations around a vertical body axis (dotted curve; right ordinate; frequency 0.03 Hz, peak velocity 135° s^{-1}). One data point corresponds to one measurement.

(ii) *Control experiments*

Unilateral removal of a statocyst. To check whether the funnel responses depend on sensory input from the statocysts, one animal with a statocyst unilaterally (right) destroyed was tested for funnel responses in the experimental set-up and, in addition, was observed and filmed in its holding tank. Before the operation, the animal showed both responses, the compensatory funnel response and the funnel follow response.

Experimental test. Six hours after unilateral statocyst removal, none of the two funnel responses were seen when the animal was tested in the experimental set-up (oscillation frequency 0.03 Hz, peak velocity 135° s^{-1}); however, the funnel showed a tonic deviation to the operated side. Eight hours after the operation, the animal was more active and a funnel follow response, but no compensatory funnel response, was seen (figure 31). During four oscillations, the funnel position curve was about 180° out of phase with the stimulus velocity curve and was shifted to the operated side. During the first oscillation, the maximal funnel position was very high (more than 60°) during counterclockwise rotations (i.e. rotations to the un-operated side). During the following three oscillations, the amplitude declined and an offset occurred

PHILOSOPHICAL TRANSACTIONS OF THE ROYAL SOCIETY B BIOLOGICAL SCIENCES

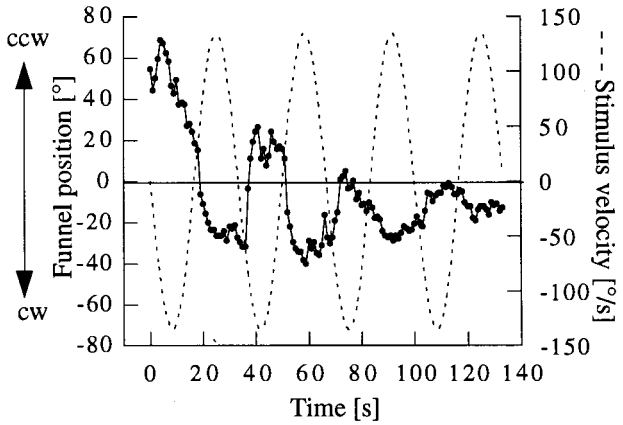

Figure 31. Funnel follow response of *Nautilus* during four sinusoidal oscillations around a vertical body axis (dotted curve; right ordinate; frequency 0.03 Hz; peak velocity 135° s^{-1}) after removal of the right statocyst. Note that the funnel middle position is shifted to the operated right (clockwise) side. One data point corresponds to one measurement.

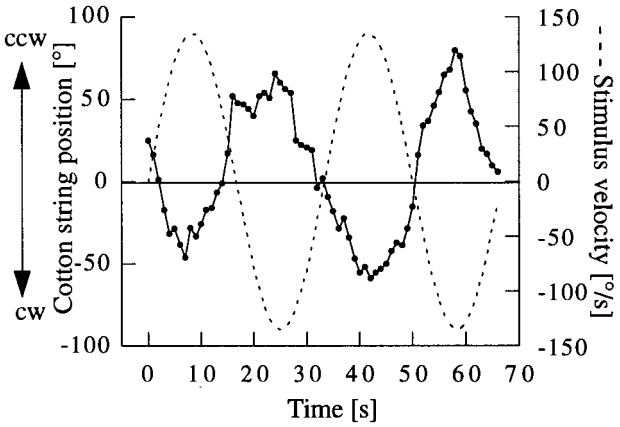

Figure 32. Passive movements of a cotton string attached to an empty *Nautilus* shell during sinusoidal oscillation around a vertical shell (= vertical body) axis (dotted curve; right ordinate; frequency 0.03 Hz; peak velocity 135° s^{-1}). One data point corresponds to one measurement.

to the operated side. When tested 24 h after the operation, the funnel follow response was similar to that of intact animals, with no offset to the operated side; however, when not oscillated, the funnel was kept towards the operated side (as seen before).

Observation of the unrestrained animal Four hours after unilateral statocyst removal, the animal was relatively inactive but showed a muscle tone asymmetry, with the funnel and tentacles kept towards the operated side. When the animal was moved by hand to the left or right around a vertical body axis, the funnel remained on the operated side. 22 h after the operation, the animal was more active and swam around in the holding tank. The muscle tone asymmetry towards the operated side was even more prominent than the day before. Most of the hood and tentacles were bent towards the operated side, as were the ipsilateral eye and the funnel which caused the animal to constantly swim in circles around its vertical body axis towards the un-operated side. Four days after the operation, the asymmetry of the muscle tone was no longer seen and the animal swam normally, with no circling.

Tests for influence of water movements. The passive rotations of the animals together with the aquarium caused complex relative movements between the animals and the water column. These water movements mainly depend on inertial forces of the water column, drag forces caused by the animal's body, and friction forces on the aquarium wall. Because all these forces may have effected the funnel responses, three types of control experiments were performed; these included tests for possible (although so far unknown) epidermal mechanoreceptors that may have sensed the relative water movements and thus have caused or contributed to the funnel responses.

Some aspects of fluid dynamics in the experimental set-ups. To visualize the water movements in the experimental set-up during sinusoidal oscillations, an empty *Nautilus* shell with a cotton string attached to its anterior edge was placed into the holder. The aquarium was then oscillated the same way as it was with a live *Nautilus* (frequency 0.03 Hz, peak velocity 135° s^{-1}). During two oscillations, the positions of the free end of the cotton string were analysed and plotted together with stimulus velocity against time (figure 32). The cotton string position curve was about 180° out of phase with the stimulus velocity curve, i.e. was similar to the funnel position curve of the funnel follow response.

Oscillation of Nautilus with plexiglas barriers in the water column. Four plexiglas barriers (30 cm high; 8 cm deep; 2 mm thick) were mounted radially to the inside wall of the aquarium with an orientation of 90° to each other. The barriers divided the water column into four (though incomplete) compartments and thereby largely changed the movement of the water column relative to the aquarium during the oscillations. The funnel position of one animal was tested in this set-up during two oscillations (oscillation frequency 0.03 Hz, peak velocity 135° s^{-1}). The animal showed a compensatory funnel response with a phase lag of the funnel position curve of about 5–10° relative to the stimulus velocity curve (figure 33); this is slightly more than the phase lag of the compensatory funnel response seen without plexiglas barriers (compare figures 24 and 33). The amplitude of the funnel responses, however, was the same (compare figures 24 and 33).

Test for possible mechanoreceptors that sense water movements. In this experiment, relative water movements were produced by sinusoidally oscillating the aquarium around a stationary animal (frequency 0.03 Hz, peak velocity 135° s^{-1}). During two oscillations, the animal showed neither compensatory funnel nor funnel follow responses; its funnel remained in a middle position (figure 34).

(iii) *Optokinetic stimulation*

To investigate the influence of visual input, funnel responses of *Nautilus* were analysed during optoki-

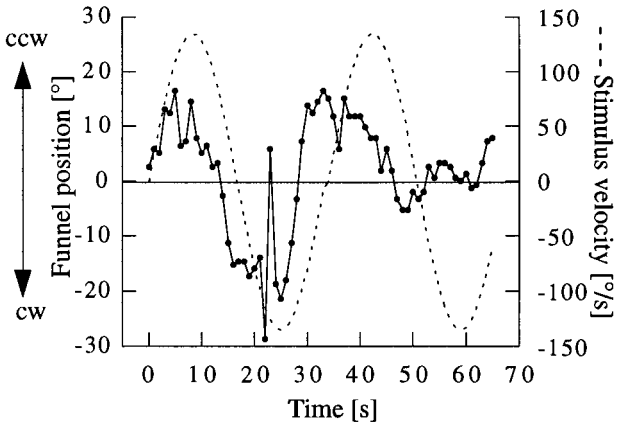

Figure 33. Compensatory funnel response of *Nautilus* during sinusoidal oscillation around a vertical body axis (dotted curve; right ordinate; frequency 0.03 Hz; peak velocity 135° s^{-1}) with plexiglas barriers that divide the water column into four compartments and thus influence the water movement. One data point corresponds to one measurement. Note that the short strong funnel movement during the second half of the first oscillation cycle most likely is due to a voluntary funnel movement.

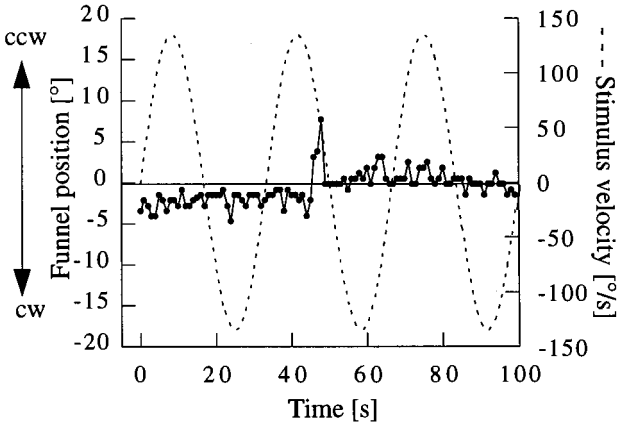

Figure 34. Funnel response of a stationary *Nautilus* during sinusoidal oscillation of the aquarium (including the water column) around a vertical body axis with the stationary animal in the axis of rotation (dotted curve; right ordinate; frequency 0.03 Hz; peak velocity 135° s^{-1}). One data point corresponds to one measurement.

netic stimulation with a black and white stripe pattern. The pattern was oscillated (frequency 0.03 Hz, stripe pattern velocity 135° s^{-1}) around the vertical body axis of stationary, restrained animals. All animals showed a clear funnel response that would have caused the unrestrained animals to follow the movement of the visual stimulus and thus would have reduced the slip of the visual image on the retina. Figure 35 shows the funnel position of a stationary animal during five sinusoidal oscillations of the stripe pattern. The direction of the funnel response during this type of stimulation is opposite to that of the compensatory funnel response during oscillations of the animal, i.e. during statocyst stimulation. The funnel position curve is periodic and is about 180° out of phase with the visual stimulus velocity curve (figure 35). The funnel position curve shows a

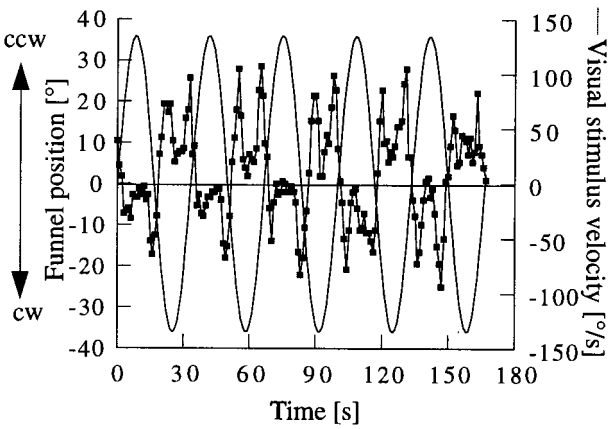

Figure 35. Compensatory funnel response of a stationary *Nautilus* during sinusoidal optokinetic stimulation with a black and white stripe pattern (spatial wavelength λ = 22.5°; pattern frequency 0.03 Hz; pattern velocity 135° s^{-1}; smooth curve; right ordinate). The funnel moves in a direction opposite to the direction of the visual stimulus, i.e. jetting would move the animal in stimulus direction. One data point corresponds to one measurement. Note that the peaks of response velocity correspond to the peaks of inverted pattern velocity.

maximum amplitude of 29°, with two distinct peaks during either part of the oscillation cycle. During the five oscillations, no obvious decline of the amplitude of the response occurred.

(iv) *Combined statocyst and optokinetic stimulation*

In this experiment, the funnel responses of *Nautilus* during optokinetic stimulation combined with statocyst stimulation were analysed (frequency 0.03 Hz, peak velocity 135° s^{-1}). The black and white stripe pattern was kept stationary outside of the aquarium and thus provided an optokinetic stimulation in a direction opposite to the direction of the oscillation of the animal (i.e. the statocyst and visual inputs were additive with regard to compensation). In addition, during two intervals (33 s and 15 s), the stripe pattern was oscillated together with the animal and thus provided a stationary cue for visual fixation (i.e. the statocyst and visual inputs were antagonistic). All animals showed a clear funnel response in the direction of animal oscillation, but opposite to the direction of visual stimulation (figure 36), i.e. for both kinds of stimulation the response is compensatory in nature. During seven oscillations the funnel position curve showed maximum amplitudes of 30–40° (in one cycle 50°), often with some kind of plateau (figure 36). The response changed when the optokinetic stimulation was stopped, i.e. the peak amplitude dropped to between 10° and 20°, indicating that the response was probably suppressed by visual fixation of the stripe pattern which was stationary relative to the animal. When the optokinetic stimulation started again, the peak amplitudes increased above 30° and the animal again showed a clear compensatory funnel response, i.e. a funnel movement in the direction of animal oscillation (=

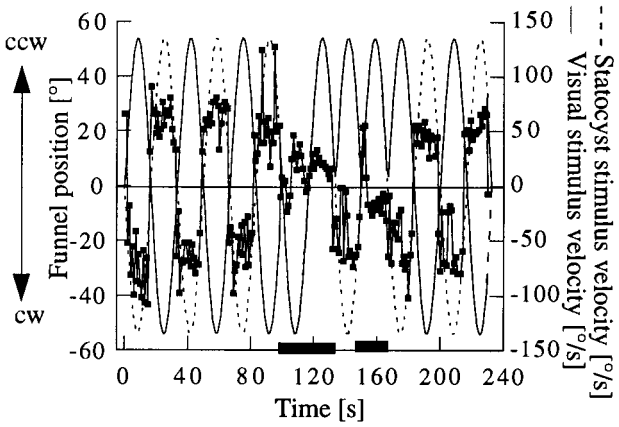

Figure 36. Compensatory funnel response of *Nautilus* during statocyst stimulation, i.e. oscillation of the animal around a vertical body axis (dotted curve; right ordinate; frequency 0.03 Hz; peak velocity 135° s^{-1}) combined with optokinetic stimulation with a stationary black and white stripe pattern (spatial wavelength λ = 22.5°; visual stimulus frequency 0.03 Hz; visual stimulus velocity 135° s^{-1}; smooth curve; right ordinate). One data point corresponds to one measurement. Black bars indicate stop of optokinetic stimulation.

statocyst stimulation) and opposite to the direction of optokinetic stimulation.

4. DISCUSSION

The morphological findings of the present study show that, based on the structure of the hair cells, the *Nautilus* statocyst can be differentiated into a dorsal and a ventral part. This, together with the fact that the hair cells are morphologically polarized, allows one to hypothesize that the statocyst is not only a gravity receptor system that detects the position of the animal relative to the direction of gravity, but is also able to detect rotatory movements (angular accelerations). This hypothesis has been confirmed by behavioural experiments that showed statocyst-driven compensatory responses of the funnel to dynamic rotation of the animal around a vertical body axis.

(*a*) *Anatomy*

(i) *Function of the statocyst*

The *Nautilus* statocyst is half filled with endolymph and half with free-moving statoconia. The borderline between the two hair cell types (type *A* and type *B*) creates an equator that approximately corresponds to the borderline between the statoconia and the endolymph when the animal is in its normal upright position. Thus, in the normal range of animal positions, the two types of receptor hair cells will be stimulated differently and this is likely to reflect a functional specialization. Type *A* hair cells in the ventral half of the statocyst will be statically stimulated by a deflection of their kinocilia due to the gravity-dependent force of the statoconia onto the sensory epithelium; thus type *A* hair cells will detect positions of an animal relative to gravity. Since changes in position will change the population of stimulated hair cells (i.e. hair cells in contact with statoconia), information about position in space is encoded in the spatial orientation of the population of stimulated hair cells (Budelmann 1975). Since type *A* hair cells are morphologically polarized, it is possible that they provide additional information about stimulus direction. Conversely, type *B* hair cells in the dorsal half of the statocyst are not in contact with statoconia but with endolymph and, therefore, will be stimulated by a deflection of their kinocilia due to endolymph movements. Consequently, angular accelerations of an animal around a vertical body axis (on a horizontal turntable) will dynamically stimulate both type *A* and type *B* hair cells at the same time (because inertia causes a movement of both the statoconia and the endolymph relative to the hair cells). This situation is different from the situation that occurs during positional changes of an animal relative to gravity because during horizontal turntable rotations the populations of stimulated hair cells (that is, the hair cells that are in contact with either the endolymph or the statoconia) remains the same. In addition, because the specific weight of the statoconia is higher than that of the endolymph, for any given angular acceleration the relative movement between the statoconia and type *A* hair cells is larger than the relative movement between the endolymph and type *B* hair cells. Because both type *A* and type *B* hair cells are polarized and consequently able to detect the directions of these relative movements, they should be able to sense angular accelerations. Furthermore, type *A* hair cells may have a lower threshold for angular accelerations than type *B* hair cells; however, physiological experiments are necessary to verify this point.

Among aquatic invertebrates, sensitivity to gravity has been reported in almost all phyla (see Budelmann 1988). In contrast, detection of angular acceleration via statocysts is known only in the most swiftly moving invertebrates, i.e. in decapod crustaceans and coleoid cephalopods (Young 1960; Markl 1974; Budelmann 1976; Sandeman 1976). In the statocysts of decapod crustaceans, cuticular hair sensilla are part of either a true canal system (crabs) or protrude freely into a cyst cavity (lobsters; see Budelmann 1988). In coleoid cephalopods a crista/cupula-system with hair cells exists that detect angular accelerations (Barber 1966; Budelmann 1970, 1976, 1977, 1988; Stephens & Young 1982; Williamson & Budelmann 1985*b*; Young 1989).

(ii) *Sensitivity of the statocyst*

The *Nautilus* statocyst contains a large number of receptor cells, a large number of statoconia and a large volume of endolymph. This suggests, that the organ is well suited to detect small positional changes and small rotatory movements.

It has been shown for the vertebrate semicircular canals (see Wilson & Jones 1979) and the statocysts of coleoid cephalopods (Maddock &Young

1984) that the larger the dimensions of the organ and the larger its inertial mass (endolymph), the more sensitive is the organ to slow rotatory movements. Consequently, slow moving animals, in general, have equilibrium receptor organs of large dimensions, whereas in fast moving animals the organs are relatively small. In coleoid cephalopods, large statocysts with a presumably high sensitivity for slow locomotion occur in buoyant, and thus slow moving, deep-sea species (Maddock & Young 1984).

The different degree of complexity and differentiation of cephalopod statocysts (*Nautilus*, octopods and decapods) correlates well with the complexity of the animals' locomotion. Decapod cephalopods are the most swiftly moving cephalopods and their statocysts, in general, show the highest degree of differentiation (see Budelmann 1990). They are of irregular shape with cartilaginous lobes (anticristae, hamuli) that protrude into the cyst cavity and direct the endolymph flow; in some species they form almost canals (Stephens & Young 1982; Young 1989). Four crista/cupula segments detect angular accelerations and three macula/statolith (statoconia) systems detect positions relative to gravity (Budelmann 1990; Williamson 1991). In octopods, on the other hand, locomotion is slower (crawling and slow swimming) and, therefore, their statocysts are less complex. They are sphere like and have only one macula/statolith system (Young 1960); their crista/cupula system, however, has nine segments and is subdivided into two systems of different sensitivity presumably to detect angular accelerations during slow crawling as well as faster swimming (Young 1960; Williamson & Budelmann 1985*a*, *b*; Budelmann *et al.* 1987*a*, *b*). *Nautilus* shows the lowest level of mobility (Chamberlain 1990) and its statocysts are the least differentiated, with no obvious gross morphological expression of an angular acceleration system such as is known in its coleoid relatives. As shown in this study, such a differentiation is present, however, at a level beyond gross morphology. In addition, as compared to other invertebrate statocysts of similar structure, the very large number of receptor cells in the *Nautilus* statocyst provides a high spatial resolution of positional changes relative to gravity.

(iii) *The Nautilus statocyst as an evolutionary intermediate state*

The gross morphology of the *Nautilus* statocyst is different from that of coleoid cephalopods but similar to statocysts of other molluscs, such as bivalves, scaphopods and gastropods (Markl 1974; Budelmann 1976, 1988). Some criteria of its structure allow one to discuss it as an evolutionary intermediate state between that of coleoid cephalopods and that of all the other molluscs. For example, gastropod statocysts are spherical and contain a single statolith or many free-moving statoconia and their inside wall is lined with 13 large (prosobranchs) or numerous small (ophistobranchs) hair cells (see Budelmann 1988); however, no gastropod (or bivalve and scaphopod) statocyst has the size and number of small hair cells, and thus the spatial resolution, as the *Nautilus* statocyst. Only the statocyst of the prosobranch gastropod *Pomacea paludosa* (although much smaller) has some similarity with the *Nautilus* statocyst since it is lined with several thousand (presumably; see Budelmann 1988) polarized hair cells (Stahlschmidt & Wolff 1972); however, it has no distinction into different hair cell types. Such a distinction exists in the statocysts of the ophistobranch gastropod *Rostanga pulchra*: it has four polarized hair cells in its ventral floor (and a compact statolith attached to their kinocilia) and six non-polarized hair cells in its dorsal roof (Chia *et al.* 1981). Also in the bivalve *Pecten* polarized and non-polarized hair cells occur in one statocyst, but they are mixed and not separately arranged (Barber & Dilly 1969). Based on their gross morphology, to date all gastropod and bivalve statocysts have been described to serve as gravity receptor systems only; however, whether those that contain polarized hair cells are additionally sensitive to angular accelerations has not yet been shown.

It is not clear why in *Nautilus* the arrangement of the cilia of the morphologically polarized hair cells is either in a regular row (type *A* hair cell) or irregular (type *B* hair cell). It can be speculated that the irregular arrangement represents an evolutionary intermediate state between the non-polarized hair cells of most gastropods and bivalves (with the kinocilia scattered or arranged in circles) and the polarized hair cells of coleoid cephalopods (with the kinocilia arranged in rows). Polarized mechanoreceptive hair cells with an irregular arrangement of kinocilia (similar to type *B* hair cell) are rare in coleoid cephalopods; they are known only in the lateral line analogue organ of *Sepia* (Budelmann, unpublished work). In most gastropod and bivalve statocysts the kinocilia are arranged in circles. Since their basal feet are oriented radially towards the centre (gastropods), or the periphery (bivalves), of the cell surface, they are described as non-polarized (see Budelmann 1976). Such non-polarized hair cells are exclusively involved in the detection of the direction of gravity. In contrast, polarized hair cells are part of either gravity or angular acceleration receptor systems; the latter systems contain exclusively polarized hair cells. In *Nautilus*, the arrangement of kinocilia in an elongated row (type *A* hair cell) is similar to that found in the polarized hair cells of the statocysts of coleoid cephalopods (*Octopus, Sepia* and *Loligo*; Barber 1968; Budelmann *et al.* 1973, 1987*a*; Budelmann 1979, 1988), and as well in the neck receptor organ of the squid *Lolliguncula* and presumably of other decapods (Preuss & Budelmann 1995*a*).

(iv) *Morphological polarization*

Type *A* and type *B* hair cells in the *Nautilus* statocyst are morphologically polarized according to the uniform orientation of the basal feet of their kinocilia; this indicates a directional sensitivity of the hair cells (see Budelmann 1979). The orientation of the basal feet is the same in neighbouring hair cells and thus

PHILOSOPHICAL TRANSACTIONS OF THE ROYAL SOCIETY B BIOLOGICAL SCIENCES

creates a specific pattern of polarization throughout the statocyst. Other morphological features that underline the polarization of the *Nautilus* hair cells are: (i) the eccentric (peripheral) position of the kinocilia on the cell surface, with the basal feet pointing towards the centre; and (ii) in type *A* hair cells the inclination of the kinocilia towards the cell surface, with the basal feet pointing away from the angle of inclination (similar as in coleoid cephalopods, see Budelmann (1979)); both features are the same in all neighbouring hair cells. It has been shown for the hair cells in the statocysts of coleoid cephalopods that such a morphological polarization has a physiological correlate: shear (deflection) of the kinocilia in the direction of their basal feet causes maximal excitation of the hair cells, and maximal inhibition when shear occurs in the opposite direction (see Budelmann 1970; Budelmann & Williamson 1994). A similar correlation has been shown for the vertebrate vestibular and lateral line hair cells (e.g. Flock 1965, 1971; Löwenstein 1974; Platt 1977). Thus, by analogy with those results, the hair cells in the *Nautilus* statocyst can be described as polarized mechanoreceptors that provide information about the direction of linear and angular accelerations.

(v) *Innervation*

As is common for invertebrate receptor cells, the hair cells in the *Nautilus* statocyst are primary sensory cells, i.e. they carry an axon. This is different from the situation in the fast moving coleoid cephalopods where the receptor epithelia are composed of, or include, secondary sensory cells (without an axon) which allow signal convergence from several receptor cells onto one first-order afferent neuron (Klein 1932; Budelmann 1976, 1977; Budelmann & Thies 1977; Colmers 1981; Budelmann *et al.* 1987*a*).

In the *Nautilus* statocyst, the organization of the nerve plexus underneath the sensory epithelium is quite complex. The plexus includes vesicle-filled profiles that most likely are part of an efferent innervation. The vesicles are clear or filled with electron-dense material. Morphological criteria that define a chemical synapse (such as an accumulation of synaptic vesicles and electron-dense pre- and post-synaptic membranes) were occasionally seen; however, so far no efferent synapses beyond doubt were found in the TEM sections examined. In coleoid cephalopods, different types of synaptic vesicles (clear and dense-core) have been described and associated with different types of transmitters (Budelmann & Bonn 1982; Auerbach & Budelmann 1986; Williamson 1989; Tu & Budelmann 1994).

In invertebrate statocysts, an efferent innervation has been described in ctenophores (Krisch 1973) and some gastropods (Wolff 1970; Janse *et al.* 1988); it is unusually high in statocysts of coleoid cephalopods, where it is thought to keep the hair cells in their best operating range by mostly inhibitory (and few excitatory) functions (Colmers 1981; Budelmann *et al.* 1987*b*; Williamson 1985, 1989; Williamson & Chrachri 1994).

As shown by silver stainings, the statocyst nerve enters the brain at the level of the magnocellular lobe and projects to the subesophageal brain cord (Young 1965). However, other neuroanatomical tracer techniques (e.g. cobalt iontophoresis or staining with fluorescent dyes) are necessary to more precisely analyse the termination of the afferent and the origin of the efferent fibres.

No innervation has been found for the ciliated cells of the *Nautilus'* Kölliker's canal. Most likely, therefore, they are non-sensory, as it is the case for the ciliated cells of the Kölliker's canal of coleoid cephalopods (Young 1960; Stephens & Young 1982); but more details of the cellular organization and observation of live tissue are necessary to verify this point. In *Nautilus*, as in decapod cephalopods, the Kölliker's canal opens to the exterior, whereas in octopods it is closed peripherally (Young 1960). In all coleoid cephalopods, the cilia in the canal are known to be motile (Budelmann 1988). In vertebrates, a similar canal-like opening to the exterior is known in the vestibular organ of lampreys and some elasmobranchs; its multi-ciliated epithelial cells are described as non-innervated and their cilia as motile (Löwenstein *et al.* 1968; Löwenstein 1974; Popper & Hoxter 1987).

(*b*) *Funnel responses*

In the behavioural experiments, *Nautilus* showed two types of funnel responses to imposed rotatory movements (angular accelerations) around a vertical body axis. The characteristics of the funnel responses are stimulus dependent and one of the funnel responses is compensatory in nature. Consequently, *Nautilus* can sense not only changes of position relative to the direction of gravity (Hartline *et al.* 1979) but also its own (at least horizontal) rotational movements. The most likely receptor organ for the detection of angular accelerations is the statocysts and this idea is supported by the data obtained after unilateral statocyst removal.

Statocysts in fast moving invertebrates, such as coleoid cephalopods and decapod crustaceans, are known to control behavioural responses to rotational movements via specialized receptor systems for angular accelerations. When dynamically stimulated on a horizontal turntable, *Octopus* and *Sepia* show compensatory movements of the eyes (postrotatory nystagmus), head and body that depend on the angular acceleration receptor system (crista/cupula system) within the statocysts (Dijkgraaf 1961; Collewjin 1970; Messenger 1970) and decapod crustaceans compensate for oscillations around a vertical body axis with eye reflexes (including post-rotatory nystagmus) that are controlled by cuticular sensory hairs in the statocyst canals (Sandeman & Okajima 1972). In vertebrates, the vestibulo-oculomotor, the vestibulo-cervical and the vestibulo-spinal reflexes are all well studied; their compensatory eye, neck and limb movements after stimulation of the semicircular canal receptors are known to provide stabilization of the eyes, head and body during rota-

PHILOSOPHICAL TRANSACTIONS OF THE ROYAL SOCIETY B BIOLOGICAL SCIENCES

tional movements (see Wilson & Jones 1979). Some insects evolved alternative systems to detect angular accelerations, such as the haltere system (dipterous insects) and neck receptors (dragonflies; Fränkel & Pringle 1938; Mittelstaedt 1950; Markl 1974; Nalbach & Hengstenberg 1986).

(i) *The compensatory funnel response*

The compensatory funnel response of *Nautilus* is phase-coupled with the stimulus, i.e. the changes of funnel position are sinusoidal and phase-locked with the stimulus oscillations (figures 24 and 26). The direction of the funnel response is the same as the direction of the stimulus and opposite to the direction of the water movement that occurs relative to the animal when rotated. This proves that the compensatory funnel response is an active movement of the funnel and is not passively induced by water movements.

The funnel position curve of the compensatory funnel response is nearly in phase with the stimulus velocity curve (figures 24 and 26). This suggests that the angular acceleration stimulus is transformed to a positional signal. This is similar to the oculomotor reflex of the crab *Scylla*, which expresses eye position in phase with body angular acceleration (Janse & Sandeman 1979). Although the receptors in statocysts of crustaceans are not hair cells, *Nautilus* and *Scylla* have in common that there is no cupula attached to the kinocilia and the cuticular sensory hairs, respectively, which would influence the stimulus transformation. In contrast, in the *Octopus* statocyst and in the vertebrate semicircular canals a cupula is attached to the kinocilia of the receptor hair cells and cupula displacement is in phase with body angular velocity (e.g. Mayne 1974; Wilson & Jones 1979; Williamson & Budelmann 1985*a*, *b*).

The phase relationship of the compensatory funnel response is frequency dependent with the best response at 0.03 Hz; this correlates well with *Nautilus'* slow locomotion. Its normal swimming speed ranges from 0.16–0.33 m s^{-1} (Packard *et al.* 1980; Chamberlain 1987; O'Dor *et al.* 1990; see also Hanlon & Messenger 1996) and its maximum angular velocity is 90° s^{-1} (Hartline *et al.* 1979). For the much faster moving coleoid cephalopods, quantitative data are available only for the statocysts of *Octopus*; there the two subsystems of the angular acceleration receptor organ show frequency dependent response thresholds between 0.01 and 0.17 Hz and between 0.06 and 1.6 Hz, respectively (Williamson & Budelmann 1985*a*, *b*). In the crab *Scylla*, phase-locked eye movements occur at frequencies between 0.7 and 1 Hz (Janse & Sandeman 1979).

When *Nautilus* is tilted by hand around roll and pitch axes (which includes positional changes relative to gravity), it moves its funnel such that it points into a direction opposite to the direction of tilt (Packard *et al.* 1980; Neumeister, unpublished work). When unrestrained, such funnel positions would manoeuvre the animal into a direction opposite to the direction towards which the funnel points and thus would compensate for the imposed tilt. In addition, *Nautilus* seems to compensate for rotation when dynamically rotated by hand around its yaw axis (which excludes positional changes relative to gravity; Packard *et al.* 1980). This indicates that *Nautilus* not only is able to sense positional changes relative to the direction of gravity but is also able to sense angular accelerations; this ability allows the animal to stabilize its course orientation with a space-constant body posture (see Schöne 1980).

Due to the gas-filled chambers of its shell, *Nautilus* is stabilized in both roll and pitch planes (Packard *et al.* 1980). This is not the case, however, during rotations around a yaw axis, where the animal is free to manoeuvre. In the yaw plane, the only way to stabilize body orientation is via compensatory funnel movements elicited by angular accelerations, because changes of body position relative to the direction of gravity are not involved.

For *Nautilus*, during its daily vertical migrations in front of a coral reef, the detection of rotatory movements around its vertical body axis is especially important to compensate for the passive displacements in the yaw plane caused by currents in front of the reef. In addition, information about rotatory movements can help to control gaze during locomotion towards a bioluminescent food. Since *Nautilus* maintains approximately neutral buoyancy during locomotion (Chamberlain 1987), small water jets through the funnel are a very efficient way for the animal to change position in space.

(ii) *The funnel follow response*

Besides the compensatory funnel response, *Nautilus* showed a funnel follow response during sinusoidal oscillations (figures 27 and 29). The funnel position curve of the funnel follow response is sinusoidal and phase locked with the stimulus. As compared to the compensatory funnel response, the direction of the funnel follow response is reversed (compare figures 24, 26, 27 and 29).

The funnel follow response is in the same direction as the stimulus-induced movements of the water column relative to the animal. This may explain why the amplitude of the funnel position curve during this response is higher than that of the compensatory funnel response (compare figures 24, 26, 27 and 29). It is difficult to decide, however, whether the funnel follow response is due to an active movement or whether it is passively induced by the movement of the water column (the experimental conditions do not allow a clear distinction between these two possibilities).

The control experiment with a cotton string attached to an empty *Nautilus* shell show that water movements during sinusoidal oscillation are in the same direction as the funnel follow response with no phase differences between the stimulus position curve and the cotton string (figure 32). Although indicative, this experiment has limitations because the induced water currents are to a certain extent different from those with a live animal (less drag; no

PHILOSOPHICAL TRANSACTIONS OF THE ROYAL SOCIETY B BIOLOGICAL SCIENCES

water stream ejected from the funnel) and the cotton string is not elastic and creates less drag than the funnel tissue.

Whether the funnel follow response is a voluntary movement, or caused by certain internal states, is difficult to decide; at least no conclusive differences in behaviour were seen during the compensatory funnel and the funnel follow responses. Although *Nautilus* can control the orifice of its funnel with respect to the cross-sectional area in order to fine tune jetting (Chamberlain 1987), no consistent differences were seen in the activity of the funnel muscles or in the funnel's cross sectional area during the two responses.

The possibility that the funnel follow response is elicited by visual stimuli (accidentally not excluded in the experimental set-up) can be ruled out because during optokinetic stimulation the animal's response is compensatory. Consequently, if there was an unknown optokinetic input from outside of the aquarium, this would have been additive to the statocyst input, i.e. would have resulted in a response in the opposite direction (= compensatory funnel response). If there was an unknown optokinetic input from the inside of the aquarium, this would have caused an asymmetry between the responses during the acceleration and deceleration parts of the oscillation cycles (see also below).

The biological significance of the funnel follow response is open for interpretation. The response does not compensate for passive rotations but, instead, results in a more intense turning of the animal's body in the same direction as the passive rotation. The mechanism that controls the two funnel responses is obviously bistabile and the animal can quickly switch from one response to the other (figure 30).

(iii) *Control experiments*

Unilateral removal of a statocyst caused a tonic bending of the funnel, hood, tentacles and eyes in the yaw plane towards the operated side. This offset of the funnel was superimposed on the funnel response (in this case the funnel follow response; figure 31) indicating that the statocysts are involved in the control of the funnel movement. A similar statocyst control has been described for compensatory eye movements in *Nautilus* (Hartline *et al.* 1979), *Octopus* (Dijkgraaf 1961), *Sepia* (Collewijn 1970) and crabs (e.g. Schöne 1954; Sandeman & Okajima 1973). The fact that the effect of unilateral statocyst removal was diminished 24 h after the operation suggests that compensation processes occurred. Unfortunately, bilateral removals of the statocysts to verify their control have not yet been successful.

During sinusoidal oscillations, other mechanoreceptors (besides the statocysts) or the eyes could have sensed rotational movements and thus could have caused the funnel responses; however, these possibilities are unlikely, or, at best, play not a significant role. Theoretically, epidermal mechanoreceptors in the skin of the hood, head, funnel or tentacles could have sensed movements of the water relative to the animal's body surface; to date, however, in *Nautilus* epidermal mechanoreceptors sensitive to water movements are not known. In addition, during oscillations of the water column around a stationary animal no funnel responses occurred (figure 34) and during oscillations of an animal with four plexiglas barriers inside the aquarium (which reduced the movements of the water column relative to the animal) the compensatory funnel response was not reduced but at least as strong as during experiments without the barriers (figure 33). Also internal proprioceptors are rare in cephalopods (Boyle 1976; Kier *et al.* 1985) and it is not known whether such receptors exist in *Nautilus*. But even if they do, the control experiments give no evidence that they are involved in either of the funnel responses. Also, visual inputs were excluded by the black screen on the outside of the aquarium and additionally by the black curtain around the entire set-up. However, because illumination was necessary for the video filming, small objects inside the water column, such as particles and air bubbles, could have served as optokinetic input. But the control experiments with a water column oscillating around a stationary animal does not support this idea.

(c) *Multisensory control of the funnel motor system*

(i) *Optokinetic stimulation*

Optokinetic stimulation of a restrained *Nautilus* caused a strong and consistent funnel response in a direction opposite to the direction of the visual stimulus. Therefore, if unrestrained, *Nautilus* would follow the moving striped pattern which, in turn, would reduce retinal slip. Such behaviour has already been described in free swimming animals (Muntz & Raj 1984) and a similar funnel response occurs in the squid *Lolliguncula* during optokinetic stimulation in the pitch, roll and yaw planes (Preuss, personal communication). Moreover, *Nautilus* is able to move its eyes around the eye stalk by four extraocular eye muscles (Mugglin 1939) and stimulus-dependent eye movements were seen in restrained animals during optokinetic stimulation (Neumeister, unpublished results).

The funnel position curve shows two peaks during each part of the oscillation cycle when pattern velocity is highest. This may be interpreted as visually-driven funnel saccades elicited by changes of fixation points or may be part of nystagmus-like movements. In invertebrates, edge fixation and saccadic movements of the eyes and head are known in coleoid cephalopods (Messenger 1981) and in arthropods (e.g. Varjú 1975; Sandeman 1983; Hengstenberg 1993). In *Sepia*, after-nystagmus occurs when the animal is exposed to visual and statocyst stimuli, with the nystagmus elicited by statocyst stimulation being less regular than elicited by optokinetic stimulation (Collewijn 1970). Similarly, in the crab *Scylla*, statocyst-driven eye movements are suppressed when the visual system is stimulated at the same time (Sandeman 1983).

PHILOSOPHICAL TRANSACTIONS OF THE ROYAL SOCIETY B BIOLOGICAL SCIENCES

(ii) *Combined stimulation*

During statocyst stimulation combined with optokinetic stimulation (figure 36), visual and mechanosensory inputs are additive and serve together to stabilize and control position and movement in space. In invertebrates, such multimodal convergence of sensory inputs has already been described in cephalopods and is known in arthropods as well. In the squid, *Lolliguncula*, a multimodal interaction between statocyst, visual and proprioceptive neck receptor inputs controls head-to-body position and may also play a role in locomotion (Preuss & Budelmann 1995*a*, *b*). In crabs, lobsters and insects an interaction between equilibrium receptor, visual and proprioceptive leg receptor inputs controls balance during swimming, walking and flight (e.g. Varjú & Sandeman 1982; Sandeman 1983; Neil *et al.* 1983) and in dipterous insects halter, visual and prosternal inputs control head movements (e.g. Strausfeld & Seyan 1985).

Although the eyes and the visual system of *Nautilus* are certainly not as complex as those of coleoid cephalopods and arthropods, the fact that in *Nautilus* visual and mechanoreceptive information converge for the control of locomotion in space is another contradiction to the initial thought that the eyes of *Nautilus* are a rather poor device and thus add to the enigma of the functional properties of the *Nautilus* eye (Land 1984; Messenger 1991).

We thank the Shriner's Burns Institute for use of equipment and B. Cox for technical assistance with SEM. We also thank M. Dobbins for assistance with TEM and photography, J. Koppe for help with data analysis, and D. Sinn for help with some behavioural experiments. H. N. especially thanks Professor A. A. Perachio (Galveston) for use of equipment and constant support and advice with the behavioural experiments and Professor D. Varjú (Tübingen) for critical discussions and advice. This work was supported by the Gottlieb Daimler—and Karl Benz—Stiftung. Additional support was provided by the Marine Medicine Budget of the Marine Biomedical Institute of the University of Texas Medical Branch at Galveston, and in part by NIH grant EY08312 (B.U.B.).

REFERENCES

Auerbach, B. & Budelmann, B. U. 1986 Evidence for acetylcholine as a neurotransmitter in the statocyst of *Octopus vulgaris*. *Cell Tiss. Res.* **243**, 429–436.

Barber, V. C. 1966 The fine structure of the statocyst of *Octopus vulgaris*. *Z. Zellforsch.* **70**, 91–107.

Barber, V. C. 1968 The structure of mollusc statocysts with particular reference to cephalopods. *Symp. Zool. Soc. Lond.* **23**, 37–62.

Barber, V. C. & Dilly, P. N. 1969 Some aspects of the fine structure of the statocysts of the molluscs *Pecten* and *Pterotrachea*. *Z. Zellforsch.* **94**, 462–478.

Boyle, P. R. 1976 Receptor units responding to movement in the *Octopus* mantle. *J. Exp. Biol.* **5**, 1–9.

Budelmann, B. U. 1970 Die Arbeitsweise der Statolithenorgane von *Octopus vulgaris*. *Z. Vergl. Physiol.* **70**, 278–312.

Budelmann, B. U. 1975 Gravity receptor function in cephalopods with particular reference to *Sepia officinalis*. *Fortschr. Zool.* **23**, 84–98.

Budelmann, B. U. 1976 Equilibrium receptor systems in molluscs. In *Structure and function of proprioceptors in the invertebrates* (ed. P. J. Mill), pp. 529–566. London: Chapman & Hall.

Budelmann, B. U. 1977 Structure and function of the angular acceleration receptor systems in the statocysts of cephalopods. *Symp. Zool. Soc. Lond.* **38**, 309–324.

Budelmann, B. U. 1979 Hair cell polarization in the gravity receptor system of the statocysts of the cephalopods *Sepia officinalis* and *Loligo vulgaris*. *Brain Res.* **160**, 261–270.

Budelmann, B. U. 1988 Morphological diversity of equilibrium receptor systems in aquatic invertebrates. In *Sensory biology of aquatic animals* (ed. J. Atema, R. R. Fay, A. N. Popper & W. N. Tavolga), pp. 757–782. New York: Springer.

Budelmann, B. U. 1990 The statocysts of squid. In *Squid as experimental animals* (ed. D. L. Gilbert, W. J. Adelman & J. M. Arnold), pp. 421–439. New York: Plenum.

Budelmann, B. U. & Bonn, U. 1982 Histochemical evidence for catecholamines as neurotransmitters in the statocyst of Octopus vulgaris. *Cell Tiss. Res.* **227**, 475–483.

Budelmann, B. U. & Thies, G. 1977 Secondary sensory cells in the gravity receptor system of the statocyst of *Octopus vulgaris*. *Cell Tiss. Res.* **182**, 93–98.

Budelmann, B. U. & Williamson, R. 1994 Directional sensitivity of hair cell afferents in the *Octopus* statocyst. *J. Exp. Biol.* **187**, 245–259.

Budelmann, B. U. & Young, J. Z. 1984 The statocyst-oculomotor system of *Octopus vulgaris*: extraocular eye muscles, eye muscle nerves, statocyst nerves and the oculomotor centre in the central nervous system. *Phil. Trans. R. Soc. Lond.* B **306**, 159–189.

Budelmann, B. U., Barber, V. C. & West, S. 1973 Scanning electron microscopical studies of the arrangements and numbers of hair cells in the statocysts of *Octopus vulgaris, Sepia officinalis* and *Loligo vulgaris*. *Brain Res.* **56**, 25–41.

Budelmann, B. U., Sachse, M. & Staudigl, M. 1987*a* The angular acceleration receptor system of *Octopus vulgaris*: morphometry, ultrastructure, and neuronal and synaptic organization. *Phil. Trans. R. Soc. Lond.* B **315**, 305–343.

Budelmann, B. U., Williamson, R. & Auerbach, B. 1987*b* Structure and function of the angular acceleration receptor system of *Octopus* with special reference to its efferent innervation. In *The vestibular system: neurophysiology and clinical research* (ed. M. D. Graham & J. L. Kemink), pp. 165–168. New York: Raven.

Chamberlain, J. A. 1987 Locomotion of *Nautilus*. In *Nautilus: the biology and paleobiology of a living fossil* (ed. W. B. Saunders & N. H. Landman), pp. 489–525. New York: Plenum.

Chamberlain, J. A. 1990 Jet propulsion of *Nautilus*: a surviving example of early paleozoic cephalopod locomotor design. *Can. J. Zool.* **68**, 806–813.

Chia, F. S., Koss, R. & Bickell, L. R. 1981 Fine structural study of the statocysts in the veliger larva of the nudibranch, *Rostanga pulchra*. *Cell Tiss. Res.* **214**, 67–80.

Collewijn, H. 1970 Oculomotor reactions in the cuttlefish Sepia officinalis. *J. Exp. Biol.* **52**, 369–384.

Colmers, W. F. 1981 Afferent synaptic connections between hair cells and the somata of intramacular neurons in the gravity receptor system of the statocyst of *Octopus vulgaris*. *J. Comp. Neurol.* **197**, 385–394.

PHILOSOPHICAL TRANSACTIONS OF THE ROYAL SOCIETY B BIOLOGICAL SCIENCES

Dijkgraaf, S. 1961 The statocyst of *Octopus vulgaris* as a rotation receptor. *Pubbl. Staz. Zool. Napoli* **32**, 64–87.
Flock, Å. 1965 Transducing mechanism in the lateral line canal receptors. *Cold Spring Harbor Symp. Ouant. Biol.* **30**, 133–145.
Flock, Å. 1971 Sensory transduction in hair cells. In *Handbook of sensory physiology: principles of receptor physiology* (ed. W. R. Lowenstein), vol. 1, pp. 396–441. Berlin: Springer.
Fränkel, G. & Pringle, J. W. S. 1938 Halteres of flies as gyroscopic organs of equilibrium. *Nature* **141**, 919–921.
Griffin, L. E. 1897 Notes on the anatomy of *Nautilus pompilius*. *Zool. Bull.* **1**, 147–161.
Hanlon, R. T. & Messenger, J. B. 1996 *Cephalopod behaviour*. Cambridge University Press.
Hartline, P. H., Hurley, A. C. & Lange, G. D. 1979 Eye stabilization by statocyst mediated oculomotor reflex in *Nautilus*. *J. Comp. Physiol.* A **132**, 117–126.
Hengstenberg, R. 1993 Multisensory control in insect oculomotor systems. In *Visual motion and its role in the stabilization of gaze* (ed. F. A. Miles & J. Wallman), pp. 285–298. Amsterdam: Elsevier.
Janse, C. & Sandeman, D. C. 1979 The role of the fluid-filled balance organs in the induction of phase and gain in the compensatory eye reflex of the crab *Scylla serrata*. *J. Comp. Physiol.* A **130**, 95–100.
Janse, C., Van der Wilt, G. J., Van der Röst, M. & Pieneman, A. W. 1988 Intracellularly recorded responses to tilt and efferent input of statocyst sensory cells in the pulmonate snail *Lymnea stagnalis*. *Comp. Biochem. Physiol.* A **90**, 269–278.
Kier, W. M., Messenger, J. B. & Miyan, J. A. 1985 Mechanoreceptors in the fins of the cuttlefish, *Sepia officinalis*. *J. Exp. Biol.* **119**, 369–373.
Klein, K. 1932 Die Nervenendigungen in der Statocyste von *Sepia*. *Z. Zellforsch. Mikrosk. Anat.* **14**, 481–516.
Krisch, B. 1973 über das Apikalorgan (Statozyste) der Ctenophore *Pleurobrachia pileus*. *Z. Zellforsch.* **142**, 241–262.
Land, M. F. 1984 Molluscs. In *Photoreception and vision in invertebrates*. NATO Asi Series A: Life sciences (ed. M. A. Ali), pp. 699–725. New York: Plenum.
Lowenstam, H. A., Traub, W. & Weiner, S. 1984 *Nautilus* hard parts: a study of the mineral and organic constituents. *Paleobiology* **10**, 268–279.
Löwenstein, O. E. 1974 Comparative morphology and physiology. In *Vestibular system, part 1: basic mechanisms* (ed. H. H. Kornhuber), pp. 75–120. Berlin: Springer.
Löwenstein, O. E., Osborne, M. P. & Thornhill, R. A. 1968 The anatomy and ultrastructure of the labyrinth of the lamprey (*Lampetra fluviatilis* L.). *Proc. R. Soc. Lond.* B **170**, 113–134.
MacDonald, J. D. 1855 On the anatomy of *Nautilus umbiculatus* compared with that of *Nautilus pompilius*. *Phil. Trans. R. Soc. Lond.* **145**, 277–288.
MacDonald, J. D. 1857 Further observations on the anatomy and physiology of *Nautilus*. *Proc. R. Soc. Lond.* B **8**, 380–382.
Maddock, L. & Young, J. Z. 1984 Some dimensions of the angular acceleration receptor systems of cephalopods. *J. Mar. Biol. Ass. UK* **64**, 55–79.
Markl, H. 1974 The perception of gravity and angular acceleration in invertebrates. In *Handbook of sensory physiology. Vestibular system, part 1: basic mechanisms* (ed. H. H. Kornhuber), pp. 17–74. Berlin: Springer.
Mayne, R. 1974 A systems concept of the vestibular organs. In *Handbook of sensory physiology. Vestibular system, part 2: psychophysics applied aspects and general interpretations* (ed. H. H. Kornhuber), pp. 494–580. Berlin: Springer.
Messenger, J. B. 1970 Optomotor responses and nystagmus in intact, blinded and statocystless cuttlefish (*Sepia officinalis* L.). *J. Exp. Biol.* **53**, 789–796.
Messenger, J. B. 1981 Comparative physiology of vision in molluscs. In *Handbook of sensory physiology. Vision in invertebrates VII/6 C* (ed. H. Autrum), pp. 93–200. Berlin: Springer.
Messenger, J. B. 1991 Photoreception and vision in molluscs. In: *Evolution of the eye and the visual system* (ed. J. R. Cronly-Dillon & R. L. Gregory), pp. 364–397. London: McMillan.
Messenger, J. B., Nixon, M. & Ryan, K. P. 1985 Magnesium chloride as an anesthetic for cephalopods. *Comp. Biochem. Physiol.* **82**, 203–205.
Mittelstaedt, H. 1950 Physiologie des Gleichgewichtssinnes bei fliegenden Libellen. *Z. Vergl. Physiol.* **32**, 422–463.
Morris, C. C. 1989 Preliminary observations on the ultrastructure of statoliths from *Nautilus*. *J. Ceph. Biol.* **1**(1), 15–20.
Mugglin, F. 1939 Beiträge zur Kenntnis der Anatomie von *Nautilus macromphalus*. *G. B. Sow. Vierteljahrschr. Naturf. Ges. Zürich* **84**, 25–118.
Muntz, W. R. A. & Raj, U. 1984 On the visual system of *Nautilus pompilius*. *J. Exp. Biol.* **109**, 253–263.
Murphy, J. A. 1978 Non-coating techniques to render biological specimens conductive. *Scan. Electr. Microsc.* **11**, 175–194.
Nalbach, G. & Hengstenberg, R. 1986 Die Halteren von *Calliphora* als Drehsinnesorgan. *Verh. Dtsch. Zool. Ges.* **79**, 229.
Neil, D. M., Schöne, H., Scapini, F. & Miyan, J. A. 1983 Optokinetic responses, visual adaptation and multisensory control of eye movements in the spiny lobster, *Palinurus vulgaris*. *J. Exp. Biol.* **107**, 349–366.
O'Dor, R. K., Wells, J. & Wells, M. J. 1990 Speed, jet pressure and oxygen consumption relationships in free-swimming *Nautilus*. *J. Exp. Biol.* **154**, 383–396.
Packard, A., Bone, Q. & Hignette, M. 1980 Breathing and swimming movements in a captive *Nautilus*. *J. Mar. Biol. Ass. UK* **60**, 313–327.
Platt, C. 1977 Hair cell distribution and orientation in goldfish otolith organs. *J. Comp. Neurol.* **172**, 283–298.
Popper, A. N. & Hoxter, B. 1987 Sensory and non-sensory ciliated cells in the ear of the sea lamprey, *Petromyzon marinus*. *Brain Behav. Evol.* **30**, 43–61.
Preuss, T. & Budelmann, B. U. 1995*a* Proprioceptive hair cells on the neck of the squid *Lolliguncula brevis*: a sense organ in cephalopods for the control of head-to-body position. *Phil. Trans. R. Soc. Lond.* B **349**, 153–178.
Preuss, T. & Budelmann, B. U. 1995*b* A dorsal light reflex in a squid. *J. Exp. Biol.* **198**, 1157–1159.
Sandeman, D. C. 1976 Spatial equilibrium in the arthropods. In *Structure and function of proprioceptors in the invertebrates* (ed. P. J. Mill), pp. 485–526. London: Chapman & Hall.
Sandeman, D. C. 1983 The balance and visual systems of the swimming crab: their morphology and interaction. *Fortschr. Zool.* **28**, 213–229.
Sandeman, D. C. & Okajima, A. 1972 Statocyst-induced eye movements in the crab *Scylla serrata*. I. The sensory input from the statocyst. *J. Exp. Biol.* **57**, 187–204.
Sandeman, D. C. & Okajima, A. 1973 Statocyst-induced eye movements in the crab *Scylla serrata*. II. The re-

PHILOSOPHICAL TRANSACTIONS OF THE ROYAL SOCIETY B BIOLOGICAL SCIENCES

sponses of the eye muscles. *J. Exp. Biol.* **58**, 197–212.
Schöne, H. 1954 Statocystenfunktion und statische Lageorientierung bei dekapoden Krebsen. *Z. Vergl. Physiol.* **36**, 241–260.
Schöne, H. 1980 *Orientierung im Raum*. Stuttgart: Wissenschafliche.
Stahlschmidt, V. & Wolff, H. G. 1972 The fine structure of the statocyst of the prosobranch mollusc *Pomacea paludosa*. *Z. Zellforsch.* **133**, 592–537.
Stephens, P. R. & Young, J. Z. 1982 The statocyst of the squid *Loligo*. *J. Zool. Lond.* **197**, 241–266.
Strausfeld, N. J. & Seyan, H. S. 1985 Convergence of visual, haltere and prosternal inputs at neck motor neurons of *Calliphora erythrocephala*. *Cell Tiss. Res.* **240**, 601–615.
Tu, Y. & Budelmann, B. U. 1994 The effect of L-glutamate on the afferent resting activity in the cephalopod statocyst. *Brain Res.* **642**, 47–58.
Varjú, D. 1975 Stationary and dynamic responses during visual edge fixation by walking insects. *Nature* **255**, 330–332.
Varjú, D. & Sandeman, D. C. 1982 Eye movements of the crab *Leptograpsus variegatus* elicited by imposed leg movements. *J. Exp. Biol.* **98**, 151–173.
Wells, M. J. 1990 The dilemma of the jet set. *New Scient.* **17**, 44–47.
Williamson, R. 1985 Efferent influences on the afferent activity from the *Octopus* angular acceleration receptor system. *J. Exp. Biol.* **119**, 251–264.
Williamson, R. 1989 Secondary hair cells and afferent neurons of the squid statoyst receive both inhibitory and excitatory efferent inputs. *J. Comp. Physiol.* A **165**, 847–860.
Williamson, R. 1991 Factors affecting the sensory response characteristics of the cephalopod statocyst and their relevance in predicting swimming performance. *Biol. Bull.* **180**, 221–227.
Williamson, R. & Budelmann, B. U. 1985*a* An angular acceleration receptor system of dual sensitivity in the statocyst of *Octopus vulgaris*. *Experientia* **41**, 1321–1322.
Williamson, R. & Budelmann, B. U. 1985*b* The response of the *Octopus* angular acceleration receptor system to sinusoidal stimulation. *J. Comp. Physiol.* A **156**, 403–412.
Williamson, R. & Chrachri, A. 1994 The efferent system in cephalopod statocysts. *Biomed. Res.* **15**(1), 51–56.
Wilson, V. J. & Jones, G. M. 1979 *Mammalian vestibular physiology*. New York: Plenum.
Wolff, H. G. 1970 Efferente Aktivität in den Statonerven einiger *Landpulmonaten* (Gastropoda). *Z. Vergl. Physiol.* **70**, 401–409.
Yang, W. T., Hanlon, R. T., Lee, P. G. & Turk, P. E. 1989 Design and function of closed seawater systems for culturing loliginid squids. *Aquacul. Engng* **8**, 47–65.
Young, J. Z. 1960 The statocysts of *Octopus vulgaris*. *Proc. R. Soc. Lond.* B **152**, 3–29.
Young, J. Z. 1965 The central nervous system of *Nautilus*. *Phil. Trans. R. Soc. Lond.* B **249**, 1–25.
Young, J. Z. 1989 The angular acceleration system of diverse cephalopods. *Phil. Trans. R. Soc. Lond.* B **325**, 189–237.

Received 16 October 1996; accepted 3 January 1997

PHILOSOPHICAL TRANSACTIONS OF THE ROYAL SOCIETY B BIOLOGICAL SCIENCES